IEEE Access
Multidisciplinary | Rapid Review | Open Access Journal

Received 11 January 2023, accepted 7 February 2023, date of publication 13 February 2023, date of current version 7 April 2023.

Digital Object Identifier 10.1109/ACCESS.2023.3244687

TOPICAL REVIEW

A Recent Review on Approaches to Design Power System Stabilizers: Status, Challenges and Future Scope

DEVESH UMESH SARKAR AND TAPAN PRAKASH, (Member, IEEE)
School of Electrical Engineering, Vellore Institute of Technology (VIT), Vellore, Tamil Nadu 632014, India

Corresponding author: Tapan Prakash (tapan.prakash@vit.ac.in)

This work was supported by the Office of Dean, Academic Research VIT Uinversity Vellore.

ABSTRACT Modern power system networks are complex and subjected to several uncertainties. Due to the complexity and uncertainties involved in power system operation, the networks are prone to instabilities. Rotor-angle instability is one such issue that, if not addressed properly, may lead to system collapse. A power system stabilizer (PSS) is primarily a power oscillation damping (POD) controller used to dampen power oscillations, thereby improving rotor angle stability. The proper design of PSSs is a challenging task and is essential for the secure and reliable operation of power systems. In the past, many power system instability events occurred, resulting in cascading failures and even blackouts. In the literature, several methods are proposed for the efficient design of PSSs or POD controllers. In this contribution, a recent review on the design of PSS is presented, along with challenges and the future scope of research in this field. On the basis of this review, it can be concluded that there is ample scope for designing PSS in a more efficient and robust manner, considering several uncertainties that may occur during the operation of modern power systems.

INDEX TERMS Artificial intelligence, FACTS devices, optimization, power system stabilizer, renewable energy integration.

I. INTRODUCTION

Presently, power system networks are exceedingly complicated and non-linear due to increased interconnections between different areas and capacity expansions [1]. As a matter of consequence, the power system may experience transient events leading to cascading outages and, in turn, the total collapse of the system [2]. Thus, one of the most difficult challenges with interconnected power networks is to maintain secure and reliable operation of the power system [3]. Instability issues that may arise during operation of a power system can be classified as voltage instability, rotor angle instability, and frequency instability. Rotor-angle instability is caused when the angle separation of the rotors of different generators in a system increases beyond a permissible limit due to an unwanted transient event, which may result in increased power oscillations and lead to total collapse of the system [2]. In 1985, at the Akosombo plant in Ghana-Ivory Coast, the power system was unstable due to low-frequency oscillation (0.6-0.7 Hz), so power system stabilizer (PSS) tuning was performed in one generating plant to mitigate the problem. In order to tackle the aforementioned instability issue, power oscillation damping is inevitably required. For this purpose, PSSs are generally utilized in the power system network to provide appropriate damping of power oscillations [4]. Conventional PSSs with fixed parameters can dampen local power oscillations but are not capable of damping inter-area oscillations efficiently [1]. Therefore, several research are carried out towards the efficient design of PSSs to dampen power oscillations and are well documented in the literature.

Power oscillations occur due to rotor angle deviations between generators in the system caused by transient events like transmission line faults, increased loading, etc. The frequency range of power oscillations lies between 0.1 and 3 Hz. For local oscillations, the range of frequency is 0.7×3 Hz, and for inter-plant oscillations, the range of frequency is 0.1×0.7 Hz [5]. One of the causes of power oscillation is the presence of weak power transfer tie lines. Heavy power

The associate editor coordinating the review of this manuscript and approving it for publication was Shadi Alawneh.

TABLE 1. Major blackouts in the world.

References	Date	Size of population affected (in millions)	Country
Ref [8]	03/12/2021	21	Sri Lanka
Ref [9]	21/05/2021	10	Jordan
Ref [10]	09/01/2021	200	Pakistan
Ref [11]	17/08/2020	21	Sri Lanka
Ref [12], [13]	04/08/2019	100	Indonesia
Ref [14], [15]	07/03/2019	32	Venezuela
Ref [16]	15/11/2018	09	Indonesia
Ref [17]	21/03/2018	10	Brazil
Ref [18]	13/03/2016	21	Sri Lanka
Ref [19]	26/01/2015	140	Pakistan
Ref [20]	01/11/2014	150	Bangladesh
Ref [21]	30-31/07/2012	620	India

circulation all over grid line interfaces due to severely imbalanced regional power as well as pumped storage units in pumping operation mode seem to be common causes of power oscillations reported in the literature survey. References [6], [7]. Some power system instabilities result in a series of failures, which may lead to significant blackouts. Though PSSs are capable of damping out power oscillations to a great extent and enhancing overall stability of the whole power system but, in case of cascading events and any other severe disturbances, PSSs will not be able to prevent total voltage collapse or blackouts.

Power oscillations in earlier power systems were negligible because the generator and load were closer together and the power system was small. But, presently, the structure of a modern power system is complex due to the widespread interconnection of numerous systems. As a result, maintaining consistent stability in the grid is a major concern, and there is every likelihood of the occurrence of power oscillations that may lead to power outages [5], [7]. Throughout the world, many real-time instances of power system instability issues that resulted in total collapses or blackouts occurred. Fig 1 depicts recent events of power system instability that occurred on a year-to-year basis. Table 1 lists the total population affected by the aforementioned events. On December 3, 2021, Colombo, a city in Sri Lanka, had a blackout that affected 21 million people [8]. The outage was triggered by the breakdown of a critical transmission line, which prompted total power loss [8], [11].

Previously, on August 17, 2020, the same type of electrical blackout occurred at the Kerawalapitiya Grid-substation, affecting 21 million people [18]. On May 21, 2021, a blackout occurred in Amman, a city in Jordan's Hashemite Kingdom, affecting 10 million people. The power outage has been triggered by a technical electrical breakdown in the Jordanian-Egyptian energy interconnection, which resulted in an outage in high-voltage grid systems and a widespread power loss across the Kingdom. Jordan has experienced two power outages in the past, in 2014 and 2004, owing to a fault in one of the energy-producing stations, as well as a major power loss caused by a technical failure in the Aqaba thermal power station [9].

The biggest blackout in Pakistan history occurred on Saturday, January 9, 2021. This blackout affected Pakistan's largest cities, including residents of Karachi, Rawalpindi, Lahore, Islamabad, and Multan. Approximately 200 million people (almost 90 percent of Pakistan's population) were affected [10]. This event has occurred as a result of a malfunction in the national power distribution system in certain regions. The problem happened at 11.41 p.m. at the Guddu power plant in Sindh province, tripping the high transmission lines and causing the national power distribution system's frequency to drop from 50 Hz to zero in less than a second, forcing power plants to shut down. It was like a cascading effect that shut down the power grid, cutting off around 10,320 megawatts of electricity [19].

On August 4, 2019, a severe power outage occurred in Jakarta, Indonesia, affecting 100 million people. It has been caused by malfunctioning transmission circuits on the Ungaran-Pemalang power line in central Java, which caused voltage drops that affected electrical networks in the provinces of Jakarta, West Java, and Banten [12], [13]. Venezuela experienced blackouts on March 7, 2019, owing to the breakdown of the Simon Bolivar hydroelectric plant (Guri dam), as well as ageing infrastructure and inadequate maintenance in the state of Bolvar, which impacted 32 million people [14], [15]. In Indonesia, due to a power outage on November 15, 2018, 9 million people were affected in south Sulawesi, west Sulawesi, and sections of central Sulawesi. The blackout has been caused by interference with the Makale-Palopo transmission line [16].

One more power outage affected a large part of Brazil on March 21, 2018, impacting 10 million people, primarily in the northern and northeastern areas. The blackout has occurred due to the failure of a transmission line near the massive Belo Monte hydroelectric station [17]. Similarly, from time to time, power system instability occurs in several nations. The majority of the causes of previous blackouts have been frequency instability caused by power oscillations in the local area as well as inter-area transmission issues [7], [22].

Several preventive measures are taken to reduce the occurrence of blackouts, such as the addition of an advanced power system stabilizer in the system to eliminate power oscillations, smart grid optimization with the addition of modern technologies, the use of advanced relay systems, and so on [22], [23].

The rest of the article is structured as follows: Section II introduces the fundamentals of power system stability, including rotor angle instability, rotor angle dynamics, and an overview of conventional power system stabilizers. Section III introduces a detailed overview of control and optimization-based techniques. Section IV provides a detailed overview of a wide area-based power oscillation damping controller. Section V introduces a detailed overview

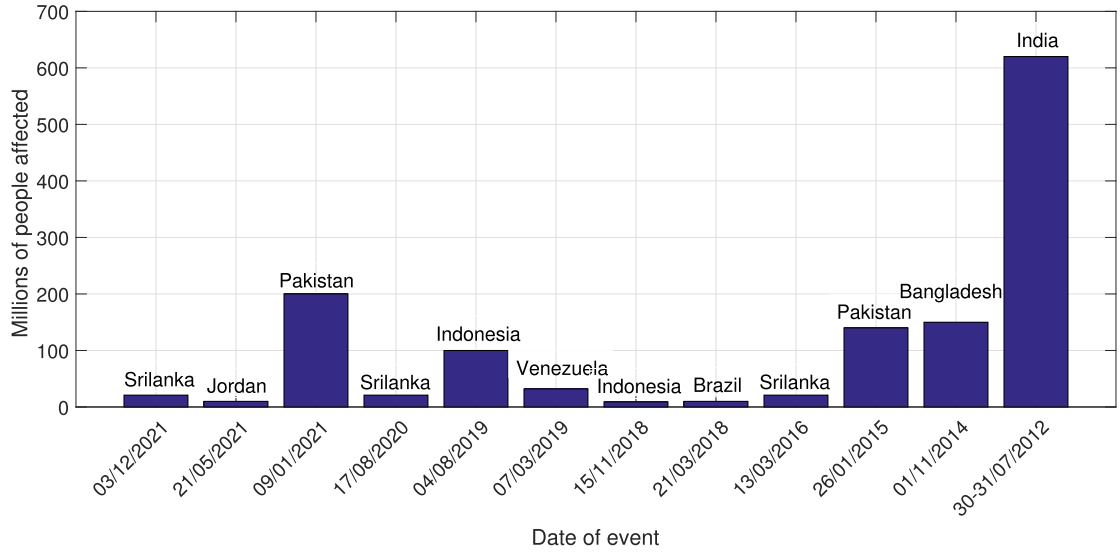

FIGURE 1. Bar chart of major blackouts in the world.

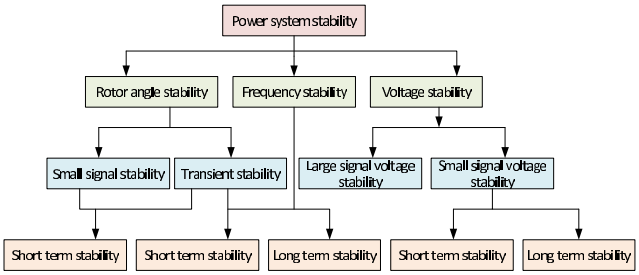

FIGURE 2. Classification of power system stability.

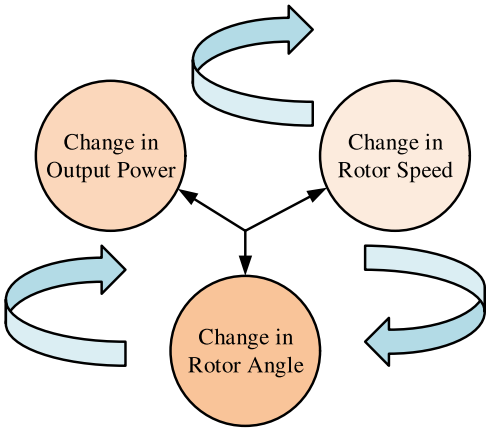

FIGURE 3. Cycle of the factors that causes power oscillations.

of the penetration of renewable sources. Section VI provides a detailed overview of FACTS devices with PSS coordination and their control. Section VII provides a detailed overview of artificial intelligence and fuzzy-based PSS coordination and their control. Finally, the concluding remarks and future challenges are illustrated in Section VIII, respectively.

II. STABILITY IN POWER SYSTEM: THE FUNDAMENTALS

The classification of power system stability is shown in Fig. 2 [1]. The key problem in sustaining the secure operation of an interconnected power system is its stability. Primarily, rotor-angle instability occurs during the transfer of power through a transmission line due to rotor-angle fluctuation between two generators caused by large perturbations at the load side. The fluctuations can be easily transferred to power, resulting in increased oscillations. Large fluctuations may lead to loss of synchronizm between generators [24]. Therefore, it is essential to dampen power oscillations in order to make the system as efficient and stable as possible [22].

A. ROTOR ANGLE INSTABILITY

Before discussing rotor angle instability, let us first define rotor angle stability, which is the capacity of a synchronous generator to retain synchronizm even after being subjected to oscillations [25]. Since the relationship between electrical and mechanical power, i.e., (P_{elec} and P_{mech}) is the same under normal operating conditions because electrical and mechanical torque, i.e., (τ_{elec} and τ_{mech}) are the same, $P_{elec} \propto \tau_{elec}$ and $P_{mech} \propto \tau_{mech}$. Here, the angular speed (ω_r) and the rated angular speed (ω_0) are equal, so that the angular rotor speed deviation ($\Delta\omega_r$) is minimal [3]. As a result, if the rotor speed deviation ($\Delta\omega_r$) is small, the synchronous generator will operate at its synchronous speed. In synchronous machines, a change in electrical torque causes disturbances that can be divided into two categories: the synchronous torque component, which is in phase with the rotor angle, and the damping torque component, which is in phase with the rotor speed deviation [2], [26].

Furthermore, rotor angle instability occurs as a small oscillation caused by consistent load changes or as a large oscillation due to severe transmission line failures [22]. The rate of change of rotor angle ($\frac{d\delta}{dx}$) is determined by the difference

between the rotor's angular speed (ω_r) and the rated angular speed (ω_0), and this difference has been referred to as the rotor speed deviation ($Deltaomega_r$). Accordingly, it can be deduced that if the rotor angle changes, the rotor speed will fluctuate, and if the rotor speed fluctuates, the generator will oscillate, and if the generator oscillates, the system may become unstable. The cycle of the factors that cause power oscillations is depicted in Fig 3 [23].

B. ROTOR ANGLE DYNAMICS

In this section, the effect of rotor angle variation and its dynamics according to the swing equation have been discussed. A synchronous machine prime mover applies a mechanical torque (τ_{mech}) to the machine shaft, and then the machine generates an electromagnetic torque. In the event of a disturbance, electromagnetic torque (τ_{elec}) is less than mechanical torque (τ_{mech}) [2], so the accelerating torque (τ_{acc}) is,

$$\tau_{acc} = \tau_{mech} - \tau_{elec} \tag{1}$$

Now, τ_{acc} has an inertia J ($kg * m^2$) which has been produced from prime mover so the equation becomes,

$$J\frac{d^2\theta_{mech}}{dt^2} = \tau_{acc} = \tau_{mech} - \tau_{elec} \tag{2}$$

where, t is time (in seconds).

We know that,

$$\theta_{mech} = \left(\frac{2}{p}\right)\theta_{elec} \tag{3}$$

where θ_{mech} is machine mechanical angle (rad), θ_{elec} is machine electrical angle (rad) and p is field poles. Now substituting Eq. (3) in Eq. (2) we get,

$$J\left(\frac{2}{p}\right)\frac{d^2\theta_{elec}}{dt^2} = \tau_{mech} - \tau_{elec} \tag{4}$$

Multiply both side by ω_{sm} in Eq. (4) we get,

$$J\left(\frac{2}{p}\right)\omega_{sm}\frac{d^2\theta_{elec}}{dt^2} = (\omega_{sm}.\tau_{mech}) - (\omega_{sm}.\tau_{elec}) \tag{5}$$

we know that,

$$\text{Electrical power } (P) = \omega_{sm}.\tau$$

where, ω_{sm} is angular speed of prime mover in mechanical quantity ($mech.rad/s$). As torque (τ) is a mechanical quantity, it has multiplied with a mechanical quantity (ω_{sm}). Then, rewrite Eq. (5) we get,

$$J\left(\frac{2}{p}\right)\omega_{sm}\frac{d^2\theta_{elec}}{dt^2} = P_{mech} - P_{elec} \tag{6}$$

Therefore,

$$J\left(\frac{2}{p}\right)\left(\frac{2}{p}.\omega_0\right)\frac{d^2\theta_{elec}}{dt^2} = P_{mech} - P_{elec} \tag{7}$$

where,

$$\omega_{sm} = \frac{2}{p}.\omega_0$$

where ω_0 is the rated angular speed. Therefore, rewrite Eq. (7) we get,

$$J\left(\frac{2}{p}\right)^2\omega_0\frac{d^2\theta_{elec}}{dt^2} = P_{mech} - P_{elec} \tag{8}$$

we know that,

$$\text{Angular momentum } (M) = J\left(\frac{2}{p}\right)^2\omega_0$$

Consequently, Eq. (8) can be written as,

$$M\frac{d^2\theta_{elec}}{dt^2} = P_{mech} - P_{elec} = P_{acc} \tag{9}$$

As per the relationship between fixed reference and rotor axis of synchronous generator, θ_{elec} is,

$$\theta_{elec} = \omega_0.t + \delta_{elec} \tag{10}$$

where δ_{elec} is electrical rotor angle in $elec.rad$. Differentiate Eq. (10) with respect to t we get,

$$\frac{d\delta_{elec}}{dt} = \omega_r - \omega_0 = \Delta\omega_r \tag{11}$$

where,

$$\omega_r = \frac{d\theta_{elec}}{dt} = \text{Angular speed of rotor } (elec.rad/s)$$

After taking double differentiation of Eq. (10) we get,

$$\frac{d^2\theta_{elec}}{dt^2} = \frac{d^2\delta_{elec}}{dt^2} \tag{12}$$

Substitute Eq. (12) in Eq. (9) to get,

$$M\frac{d^2\delta_{elec}}{dt^2} = P_{mech} - P_{elec} = P_{acc} \tag{13}$$

Hence, Eq. (13) is called as swing equation. The above equation states that, if a system is to be stable during disturbances, the rotor angle must oscillate around an equilibrium point. Furthermore, if the rotor angle continues to oscillate endlessly without reaching a new state of equilibrium, the machine is deemed to be in a transiently unstable [2], [3].

In normal operating condition, $\tau_{mech} = \tau_{elec}$ means $P_{mech} = P_{elec}$ which means $\omega_0 = \omega_r$. Therefore, it can be concluded that, under normal operating conditions, the angular rotor speed is the same as the rated angular speed of the rotor. However, if the rotor angle between two generators fluctuates, the rotor speed will fluctuate too, resulting in rotor speed deviation. Therefore, rotor angle must be maintained within a permissible limit in order to attain system stability [1], [26].

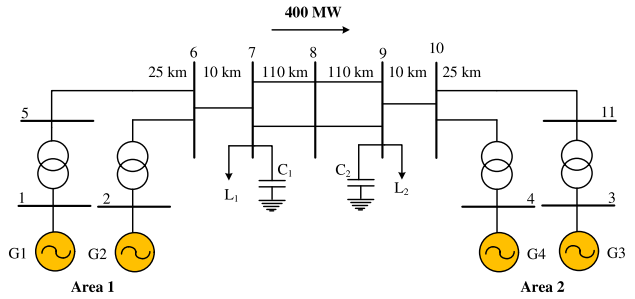

FIGURE 4. Two area 4-machine 11-bus Kundur test system.

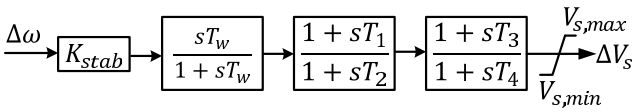

FIGURE 5. Block diagram of $\Delta\omega$ PSS.

C. OVERVIEW OF CONVENTIONAL POWER SYSTEM STABILIZER

1) SMALL SIGNAL STABILITY ANALYSIS OF MULTI-MACHINE POWER SYSTEM

Small signal stability analysis of multi-machine power system (MMPS) is discussed in this section. The fundamental approach of small signal stability analysis in context of power oscillations in power system networks are mathematically deduced below. Following are the differential equations of MMPS [27],

$$\frac{d\delta_{elec,i}}{dt} = \omega_{r,i} - \omega_0 = \Delta\omega_{r,i} \tag{14}$$

$$\frac{d\omega_{r,i}}{dt} = \frac{\tau_{m,i}}{G_i} - \frac{E'_{q,i}I_{q,i}}{G_i} - \frac{(x_{q,i} - x'_{d,i})}{G_i} I_{d,i}I_{q,i} - \frac{D_i(\omega_{r,i} - \omega_0)}{G_i} \tag{15}$$

$$\frac{dE'_{q,i}}{dt} = -\frac{E'_{q,i}}{\tau'_{d0,i}} - \frac{(x_{d,i} - x'_{d,i})}{\tau'_{d0,i}} I_{d,i} + \frac{V_{fd,i}}{\tau'_{d0,i}} \tag{16}$$

$$\frac{dV_{fd,i}}{dt} = -\frac{V_{fd,i}}{\tau_{A,i}} + \frac{K_{A,i}}{\tau_{A,i}}(V_{ref,i} - V_{t,i} + V_{s,i}) \tag{17}$$

where, $\Delta\omega_{r,i}$ is angular rotor speed deviation of i^{th} generator. As G_i is the gain of i^{th} generator and $E'_{d,i}$ and $E'_{q,i}$ are the voltages proportional to d-axis and q-axis flux linkages of i^{th} generator, respectively. $I_{d,i}$ and $I_{q,i}$ are the direct and quadrature axis currents of i^{th} generator and $x_{d,i}$ and $x_{q,i}$ are the direct and quadrature axis synchronous reactances of i^{th} generator, respectively. $\tau'_{d0,i}$ is the transient open circuit time constant of i^{th} generator. $x'_{d,i}$ and $x'_{q,i}$ are the direct and quadrature axis transient reactances of i^{th} generator, respectively. $V_{fd,i}$ is the field voltage of i^{th} generator. $K_{A,i}$ and $\tau_{A,i}$ are the AVR gain and time constant of i^{th} generator, respectively. $V_{t,i}$ is the terminal voltage of i^{th} generator and $V_{s,i}$ is the output of PSSs of i^{th} generator.

If the terminal voltage for direct axis component is $V_{td,i} = V_{t,i}sin(\delta_i - \theta_i)$ and for quadrature axis component is $V_{tq,i} = V_{t,i}cos(\delta_i - \theta_i)$ then the electrical output power is,

$$P_{elec,i} = E'_{d,i}I_{d,i} + E'_{q,i}I_{q,i} - (x'_{d,i} - x'_{q,i})I_{d,i}I_{q,i} \tag{18}$$

Consequently, the network equations are represented in the network reference frame as,

$$[I] = [Y_N][V] \tag{19}$$

where, $[I]$ and $[V]$ are the current and voltage vectors in the network reference frame with the components $(I_{D,i} + jI_{Q,i})$ and $(V_{D,i} + jV_{Q,i})$ $(i = 1, \ldots..m)$, respectively. Network bus admittance matrix is denoted by $[Y_N]$.

Therefore,

$$\begin{bmatrix} I_{D,1} + jI_{Q,1} \\ . \\ . \\ . \\ I_{D,m} + jI_{Q,m} \end{bmatrix} = [Y_N] \begin{bmatrix} V_{D,1} + jV_{Q,1} \\ . \\ . \\ . \\ V_{D,m} + jV_{Q,m} \end{bmatrix} \tag{20}$$

To understand the concept of power oscillation damping in MMPS more clearly, the Kundur two-area, four-machine, 11-bus system illustrated in Fig. 4 is examined. For damping power oscillation, Multi-band PSS (MB-PSS) and Delta ω PSS are preferred for power oscillation damping due to the fact that their input is rotor angular speed deviation $(\Delta\omega_r)$. The structures of Delta ω PSS and MB-PSS are depicted in Fig. (6) and Fig. (5), respectively. To comprehend the behaviour of CPSS present in the system, some simulation results of the system are obtained, as shown in Fig. (7). The results in the figure show that in a system without PSS, oscillations are extreme, which means that the system becomes unstable and there is a maximum possibility of a power outage. The peak overshoot, peak undershoot, and curve shape of the MB-PSS are superior to those of $\Delta\omega$-PSS. Furthermore, the damping strength of MB-PSS is greater than $\Delta\omega$-PSS in single-line-to-ground fault conditions. MB-PSS stabilizes power oscillations more quickly and efficiently compared to $\Delta\omega$-PSS.

2) INCLUSION OF PSS IN EXCITATION SYSTEM

The system provides additional dynamics if a PSS is used [27].

$$\frac{dx_{t_1}}{dt} = \frac{1}{\tau}\left[K_{stab}\Delta\omega_r - x_{t_1}\right] \tag{21}$$

$$\frac{dx_{t_2}}{dt} = \frac{1}{\tau_2}\left[K_{stab}\frac{\tau_2 - \tau_1}{\tau_2}\Delta\omega_r - \frac{\tau_2 - \tau_1}{\tau_2}x_{t_1} - x_{t_2}\right] \tag{22}$$

$$\frac{dx_{t_3}}{dt} = \frac{1}{4}\left[K_{stab}\frac{\tau_1}{\tau_2}\frac{(\tau_4 - \tau_3)}{\tau_4}\Delta\omega_r - \frac{\tau_1}{\tau_2}\frac{(\tau_4 - \tau_3)}{\tau_4}x_{t_1} + \frac{(\tau_4 - \tau_3)}{\tau_4}x_{t_2} - x_{t_3}\right] \tag{23}$$

where, K_{stab} is the stabilizing gain of PSS and x_{t_1} and x_{t_2} are used as intermediate variables. The aforementioned equations

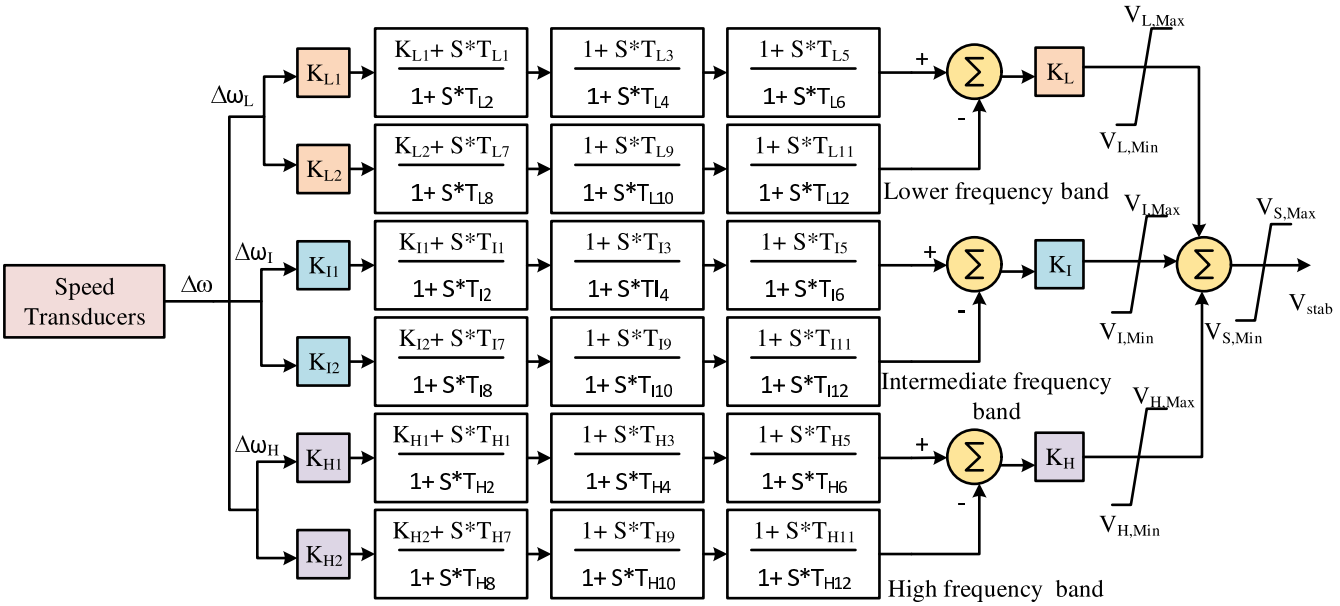

FIGURE 6. Block diagram of multiband PSS.

are augmented differential equations from Eq. (14) to Eq. (17) for each machine. If there is only one stage in the lead-lag network, Eq. (23) can be eliminated by setting $\tau_3 = \tau_4$ and $x_{t_2} = x_{t_3}$ [27]. Then the following equations are formed:

$$\frac{dx_{t_1}}{dt} = \frac{1}{\tau}\left[K_{stab}\Delta\omega_r - x_{t_1}\right] \tag{24}$$

$$\frac{dx_{t_2}}{dt} = \frac{1}{\tau_2}\left[K_{stab}\frac{\tau_2 - \tau_1}{\tau_2}\Delta\omega_r - \frac{\tau_2 - \tau_1}{\tau_2}x_{t_1} - x_{t_2}\right] \tag{25}$$

Consequently, the linearized output of a two-stage PSS is given by,

$$\Delta V_s = x_{t_3} + \frac{\tau_{t_3}}{\tau_{t_4}}\left(x_{t_2} + \frac{\tau_1}{\tau_2}\right) - x_{t_1} + K_{stab}\Delta\omega_r \tag{26}$$

Thus, the output of PSS with a single stage is given by,

$$\Delta V_s = x_{t_2} + \frac{\tau_1}{\tau_2}\left(-x_{t_1} + K_{stab}\Delta\omega_r\right) \tag{27}$$

where, ΔV_sÂ is the change in stabilizing voltage signal which is the output signal of the PSS and fed into the excitation system.

III. CONTROL AND OPTIMIZATION BASED TECHNIQUES

Control-based techniques require exact configuration of the system, whereas optimization techniques, which require additional computational time and a well-formulated objective function, are proposed in [28]. In [29], a decentralized proportional integral derivative (PID)-PSS has been developed using an iterative method based on linear matrix inequality (LMI) techniques.

In [30], two iterative LMI techniques have been proposed to examine the problem of quadratic stability in polytopic systems with the utilization of static output feedback (SOF) controllers. H_2 controller-based LMI technique designed to damp low-frequency oscillation (LFO) has been proposed in [31]. Here, the damping performance of this controller is superior to that of CPSS across a wide range of conditions. PSS is designed in [32] on the basis of a linear optimum feedback controller (LOFCD), which has been proposed to provide a step-by-step process for deriving PID parameters without the use of the trial-and-error (TAR) method.

For designing PSS, [33] proposed a system identification method based on determining the Eigenvalue Sensitivity Function. This technique calculates the effect of errors in the mathematical model. Here, the automatic voltage regulator (AVR) enhances the steady-state stability of the power system. In practice, the TAR method outperforms the Zeigler-Nichols method Â [33].

In [34], a robust control technique based on the concept of loop shaping known as H_∞ robust control optimization method has been presented and then applied to the AVR-PSS system in order to optimize the transient and dynamic stability of a turbo alternator coupled to a single machine infinite bus system (SMIB). In [35], a robust PSS-based particle swarm optimization (PSO) with mixed sensitivity H_∞ is designed using the LMI method. [36] describes and designs a proportional integral (PI) PSS-based controller. This technique improves the mathematical calculation and computational time of the system. Also, a 2-level control technique is discussed in [36] to minimise the LFO. This technique is superior to the genetic algorithm (GA), PSO, bacterial foraging optimization (BFO), and some other CPSS.

To overcome the challenges of rotor-angle stability, a cascaded control approach based on a PID controller and the

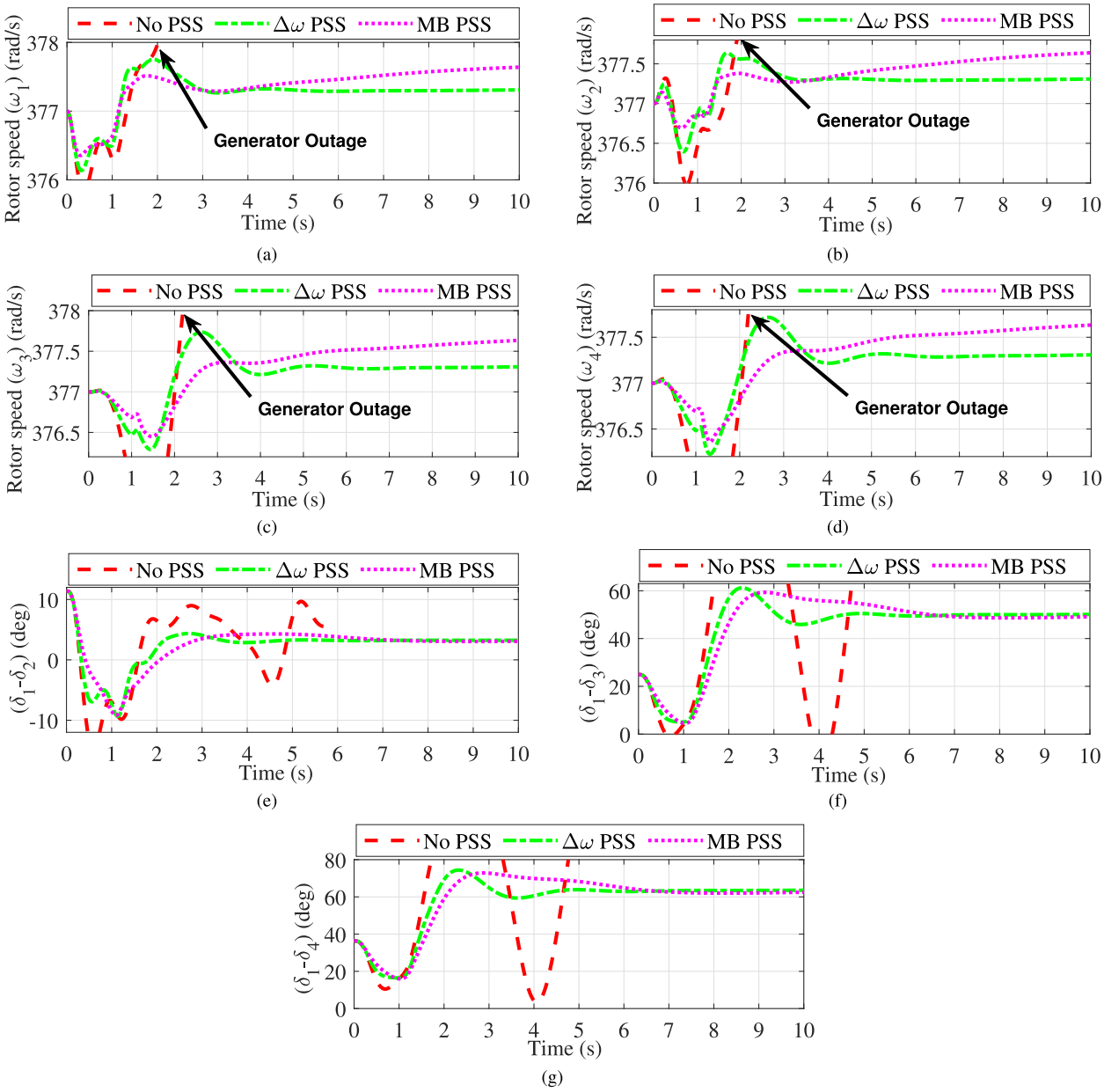

FIGURE 7. Performance of CPSS in MMPS with AG Fault. (a) Rotor speed of G_1 (ω_1). (b) Rotor speed of G_2 (ω_2). (c) Rotor speed of G_3 (ω_3). (d) Rotor speed of G_4 (ω_4). (e) Rotor angle (δ) difference between of G_1 and G_2 (*deg*). (f) Rotor angle (δ) difference between of G_1 and G_3 (*deg*). (g) Rotor angle (δ) difference between of G_1 and G_4 (*deg*).

marine predator algorithm (MPA) has been proposed in [37]. Here, MPA is more efficient and effective than traditional controllers with respect to rotor angle stability. A mechanism for explicit self-tuning control (ESTC) has been proposed in [38] to improve the stability and damping of the LFO. Here, the structure of the proposed controller, which acts as an adaptive PSS, depends on the principle of recursive least squares (RLS).

In [39], robust robust-PSS-based programming of a sequential conic has been designed to solve the problems of tuning PSS gain (TPG) and tuning PSS parameters (TPP). Here, the simulation results are tested on a 68-B test system. A CPSS-based quantum-behaved PSO has been presented in [40] in order to reliably tune PSS parameters (TPP) and mitigate the overall LFO of the system using an eigenvalue-objective function. In [41], a probabilistic PSS based on recursive GA has been designed for optimizing PSS parameters and overcoming PSS design challenges.

CPSS-based GA has been developed in [42] for effectively damping LFO and TPP. The simulation results are tested in this case using the 10M-39B New England Test System (NETS). Reference [43] proposed an improved modified PSO by passive congregation with chaos integration to design a PSS for TPP. PSS based fuzzy logic (FL) incorporation

with chaotic ant swarm optimization (CASO) technique is designed for effectively TPP has been presented in [44]. A PSS-based improved PSO algorithm designed for damping the LFO to optimize convergence speed and search space more effectively has been proposed in [45]. Here, the simulation results are tested on a 2-A test system.

A cultural algorithm (CA)-based PSS designed to dampen LFO has been presented in [46]. A modified MB-PSS technique that incorporates PSO, CA, and co-evolutionary (CE) algorithms for optimally damping LFO and TPP has been proposed in [47]. According to [48], a CPSS-based bat algorithm (BA) has been designed to tune the pole zero and gain parameters to damp an LFO.

PSS-based ant colony optimization (ACO) designed to improve the number of iterations and damping performance has been presented in [49]. Here, the simulation result is tested on the 3M-9B and 8M-36B test systems. Reference [50] proposes a honeybee mating optimization (HBMO) technique based on CPSS for optimising parameters and determining the optimal location to damp LFO. In [51], a PSS-based Cuckoo Search Algorithm (CSA) designed to increase the robustness of PSS parameters and improve the performance of the damping LFO has been presented. A PID-PSS-based BA designed to increase the robustness of PID-PSS parameters and to enhance the performance of damping LFO has been presented in [52].

PSS-based CSA is designed to enhance the damping of LFO and has been presented in [53]. Here, the robustness of the system is tested under the 3M-9B system. PSS-based PID inclusion with PSO, according to [54], is intended to optimise the parameter affected by incoming uncertainties. In [55], a robust PID-PSS-based bacterial foraging optimization (BFO) technique for inclusion with PSO has been proposed to improve the damping performance and TPP of the system. In [56], a fractional order (FO)-PID-PSS-based BA is designed to enhance the damping of LFO. In [57], modified PSO algorithms are designed to improve the TPP, and a damping LFO has been presented. Here, the simulation results are tested on the 3M-9B system.

PSS-based CSA is designed to dampen the LFO and TPP of the system by evaluating its efficacy, as presented in [58]. A controller based on a static synchronous series compensator (SSSC) typed FO-single output multi-input (SOMI) is designed for inclusion with the whale optimization algorithm (WOA) to damp out electromagnetic LFO and TPP, as well discussed in [59]. In [60], a PSS-PID-based modified PSO has been designed to reduce the influence of computation time and improve the damping performance of the system.

A damping LFO has been proposed in [61], PSS-based WOA is designed to TPP. Here, the simulation results are tested in the 3M-9B system, the 2A-4M system, and the 10M-39B NETS. In [62], a PSS-based stability non-linearity index (SN) has been designed using a newly developed SN-PSS-Hyper-spherical search (HSS) optimization algorithm to maximise the damping ratio coefficients and minimize the non-linearity index (NI) of the dominant electro-mechanical mode. Here, the simulation results are tested on the 2A-4M-11B and IEEE 10M-39B test systems. A PSS-based improved WOA has been designed in [63] to improve damping performance and finely control the PSS parameters. Here, the simulation results are tested under 3M-9B, 2A-4M, and 10M-39B NETS.

PSS based on simulated annealing (SA) and the atom search algorithm (ASO) has been designed and has been proposed in [64]. Here, the balance between the exploration and exploitation phases is excellent, with optimal TPP and damping LFO. Furthermore, the simulation results of the system are tested in the Heffronâ Phillips SMIB model, and the results are compared with PSO, GA, SA, ASO, and gravitational search algorithms (GSA). In [65], modified grey wolf optimization (GWO) is designed to improve the TPP, and damping LFO has been proposed. Table 2 shows an overview of the methodologies for PSS controller parameter tuned through optimization techniques.

IV. WIDE-AREA BASED POWER OSCILLATION DAMPING CONTROLLER

Reference [69] proposes a Wide Area Measurement System (WAMS) technique for controlling remote signals to improve LFO damping. There are two types of networks in the remote signal transmission line: communication channel (CCN) and open communication network (OCN), where CCN introduces constant delays and OCN introduces time-varying delays, as has been proposed in [70]. In [69], a unique approach for calculating the delay-dependent stability criteria on the basis of Lyapunov stability theory (LST) theory and the Schur model reduction technique (SMRT) method has been proposed to optimize the low-order system. Furthermore, LMI methods are used to achieve the delay margin with less conservatism. As discussed in [69], there is an increase in delay margin, the damping performance of a conventional wide area damping controller (WADC) degrades, and the gain margin decreases. Consequently, the simulation results are tested under 2A-4M system.

Reference [70] proposed an adaptive delay compensator (ADC) with synthesis (H_2/H_∞) approach to compensate for time delay disturbances and optimise the performance of a WADC based on WAMS. Here, the compensator is capable of successfully compensating phase angle deviations that are induced by various time delays, and the system is tested in 2A-4M and IEEE 39-Bus NETS.

In [71], a novel computation of the damping factor used to design WADC based on time delay margin has been presented. Here, LST and integral inequality methods are employed for determining the delay margin. Also, calculation speed is increased, conservatism is reduced, and the balance between signal transmission delay and damping performance is maintained in [71].

In [72], a wide area measurement system-based damping controller is designed to damp inter-area oscillation mode and compensate the remote feedback communication time delay (CTD) signal. In [73], a WADC is designed with a

TABLE 2. An overview of optimization-based methodologies for tuning of PSS controller parameters.

Reference	Design	System Dynamics	Technology	Remarks
Ref [30]	PID-PSS	SMIB	LMI techniques	Improve TPP
Ref [31]	Robust H_2 PSS	SMIB	LMI techniques	Improve damping LFO
Ref [32]	PSS	SMIB	LOFCD	Improve TPG, damping LFO
Ref [33]	PSS	SMIB	Bairstow method, eigenvalue sensitivity	Improve TPP, damping LFO
Ref [66]	PSS	SMIB	AVR, Zeigler-Nichols Method	Improve TPP, damping DLFO
Ref [34]	PSS	SMIB	AVR, H_∞ robust control optimization method	Improve TPP, damping LFO
Ref [35]	Robust-PSS	SMIB	PSO with mixed sensitivity H_∞, LMI approach	Improve TPP, damping LFO
Ref [36]	Proportional integral (PI)-PSS	SMIB, 2M, 3M	PI-controller	Improve damping LFO, structure, robustness
Ref [37]	Proportional integral derivatives (PID)-PSS	SMIB, IEEE 39-bus NETS	MPA, PID controller	Improve rotor angle stability
Ref [38]	PSS	SMIB	ESTC, PID controller, RBFNN, RLS	Improve TPP, damping LFO
Ref [39]	PSS	IEEE 68B test system	Sequential conic	Improve TPG, damping LFO
Ref [40]	CPSS	SMIB	Q-PSO	Improve TPP, damping LFO
Ref [41]	Probabilistic-PSS	3A-8M-24B	recursive GA	Improve optimal PSS design problem, TPP
Ref [42]	CPSS	10M-39B NETS	GA, linear control theory	Improve TPP, damping LFO
Ref [43]	Modified-PSO-PSS	2A test system	Passive congregation with chaos	Improve TPP, damping LFO
Ref [44]	PSS	SMIB-PSS2BAND-PSS3BAND-PSS4BAND	CASO, FL	Improve TPP, damping LFO
Ref [45]	PSS	2A test system	IPSO, AVR	Improve TPP , damping LFO searching space and convergence speed
Ref [46]	PSS	IEEE 4M-11B, 10M-39B	CA	Improve TPP, damping LFO
Ref [47]	Modified MB-PSS	MB-PSS	PSO, CA, CE	Improve TPP, damping LFO
Ref [67]	PSS	5A-16M-68B	PSO, MIADHDE, GSTHDE	Improve TPP, damping LFO
Ref [48]	CPSS	SMIB	BT	Improve TPG, TPP, damping LFO
Ref [49]	PSS	3M-9B, 8M-36B	ACO, GA	Improve damping LFO
Ref [50]	CPSS	10M-39B, 16M-68B NETS	HBMO	Improve TPP, damping LFO, find PSSs optimal location
Ref [51]	PSS	3M-9B	CSA	Improve TPP, damping LFO
Ref [52]	PID-PSS	SMIB, 2A-4M-10B, IEEE 10M-39B NETS	BA, PID controller	Improve TPP, damping LFO
Ref [53]	PSS	3M-9B	CSA	Improve TPP, damping LFO
Ref [54]	PID-PSS	SMIB	PSO	Improve TPP, damping LFO
Ref [55]	Robust-PID-PSS	SMIB	BFO, PSO	Improve TPG, damping LFO
Ref [56]	FO-PID-PSS	SMIB	BA, FO-PID	Improve TPP, damping LFO
Ref [68]	FO-PID-PSS	SMIB	GWO, GA, PSO, FO-PID	Improve TPP, damping LFO, rotor and power angle deviation
Ref [57]	PSS	PSS-4BAND 3M-9B	IPSO	Improve TPP, damping LFO
Ref [58]	PSS	10M-39B NETS	CSA	Improve TPP, damping LFO
Ref [59]	FO-SSSC-PSS	3M-6B	WOA, SSSC	Improve TPP, damping LFO
Ref [60]	PID-Modified-PSS	SMIB	PSO, PID	Improve TPG, damping LFO, reduce the complexity and computational time
Ref [61]	PSS	3M-9B, 2A-4M, 10M-39B NETS	WOA, unique hunting method	Improve TPP, damping LFO
Ref [62]	PSS	2A-4M-10B, 10M-39B NETS	Stability non-linearity index-PSS-HSS	Improve damping LFO, minimizing Non-linearity index
Ref [63]	PSS	3M-9B, 2A-4M, 10M-39B NETS	Improved-WOA	Improve-TPP, damping LFO
Ref [64]	PSS	SMIB	Improved-ASO, Simulated annealing	Improve TPP, damping LFO
Ref [65]	PSS	2A-4M-10B	Improved-GWO	Improve TPP, damping LFO

hardware-in-the-loop real-time (HILRT) simulation system to eliminate the disturbances from inter-area oscillations and to compensate the time-varying delay signal from the wide-area transmission line.

In [74], WAPSS-based synchrophasor measurement technique has been designed to damp inter-area oscillation and compensate for CTD. Here, the Jaya algorithm (JA) is used to strengthen the parameters of wide area PSS (WAPSS), and geometric measures were taken to obtain the input signal. A WADC-based power oscillation damper with time delay compensator (TDC) has been designed in [75] to reduce the attenuation effect caused by noise pollution in wide area signals.

In [76], a compact WADC with a classic-PSS structure has been designed for use with a unified residue (UR) approach to dampen the LFO with parallel balance time delay compensation (TDC) and to maintain the balance between time delays. In [77], WADC based on the LMI approach has been designed to enhance the performance of WADC. Here, uncertainties in CTD and permanent system failures occur whenever there is

a chance of a cyberattack on the phasor measurement units (PMU) of WADC channels.

In [78], a novel method of WAMS-based fractional order (FO)-PID controller as an auxiliary controller is designed for large-scale photovoltaic (PV) farms to improve the performance of LFO damping and reduce the uncertainties in system parameters. In [79], a delay margin-based PI controller has been designed for compensating and predicting accurate CTD to improve system stability. Here, a novel smith predictor (SP) based WAPSS with discrete hidden markov model (DHMM) has been developed.

Reference [80] developed a multi-objective optimization function to robustly improve WAPSS damping performance, solve small and large disturbance angular instability problems, minimise eigenvalue sensitivity to small disturbances, and vary WADC time delay. The simulation results were validated using the 16M-68B New York Power System (NYPS) and NETS. In [81], a WADC-based HY-PSO algorithm has been designed to improve the performance of the proposed system and reduce uncertainties in the operating point, variations in the time delay, and the failure of CCN due to a cyberattack. Table 3 shows an overview of the literature survey of WAPSS.

V. RENEWABLE SOURCE PENETRATION

In recent years, researchers have been attracted towards renewable energy source (RES) integration in grid-connected networks [82]. In [83], a WAPSS for a wind-integrated system incorporating stochastically tuned conventional structured phase-lead-lag to dampen or overcome the inter-area LFO as a system facing enormous stochastic variation in the steady state while determining the operating point has been designed. In [84], a PSS-based energy storage system (ESS) has been designed to choose the optimal installation location and feedback signal by dampening torque indices (DTI).

In [85], PSS-based conventional-PSO passive congregation has been designed, which is an evolutionary algorithm inclusion with doubly fed induction generators (DFIG) on wind turbines (WT) to improve LFO damping. In [86], a hierarchical wide area controller (WAC) is designed to maximise damping performance while providing a proper control signal between the synchronous generator and RES controller. A gain-scheduling WADC has been designed for the RES integration in [87] to improve the damping performance of wide area transmission line signals.Â

Reference [88] has designed a wide-area power oscillation damper (POD)-based DFIG-based wind farm to compute the gain scheduling WADC using an LMI approach and the staircase basis function method. Here, a tensor product model is converted into a linear parameter based on a parallel distributed compensation (PDC) controller. Also, it compensates the dropouts of packet data signals, CTDs, and inter-area oscillations from wide-area transmission line signals. In [89], type-II-FL based PSS has been designed to compensate the high level wind penetration. Fig 8 shows the block diagram

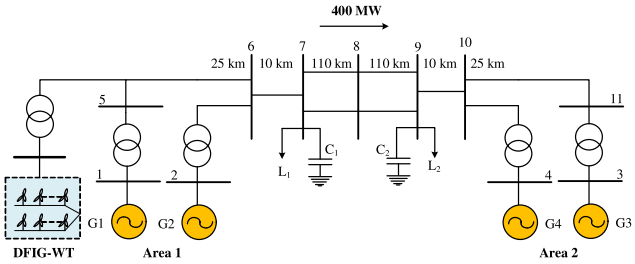

FIGURE 8. Two-area, four-machine, 11-bus test system with DFIG wind turbine integration.

of a two-area, four-machine, 11-bus test system with the integration of a DFIG wind turbine.

In [90], an optimal oscillation damping controller (OODC) based on a reduced-order model (ROM) is designed for DFIG-WT to provide appropriate control signals. In [91], an adaptive dynamics programming technique was used in the policy iteration algorithm (PIA) for DFIG-WT solved by riccati equations (ARE) to design a damping controller based on an improved efficient cubature-Kalman filter (CKF). Here, the simulation results were tested in a modified IEEE-WSCC-9B system, and the effectiveness is observed by comparing it with an optimally tuned conventional damping controller and a traditional linear quadratic regulator (LQR).

An ADC-based WADC has been designed using the synthesis $H_i nfty/H_2$ approach for the coordination of a flexible AC transmission system (FACTS) and wind farm to provide appropriate scheduling and CTD and to dampen the uncertainties from oscillations, as proposed in [92]. In [93], the effect of incorporating power oscillation damping and an inertia controller into the structure of the WT system has been examined. This will affect the drivetrain, blades, and tower and also have a marginal effect on POD performance. The simulation results are validated using a 2A-4M-11B test system equipped with a full-scale converter (FCT)-WT.

In [94], a Youla-Kucera-polytopic linear parameter varying (LPV) has been designed for DFIG integrated with the power grid and virtual inertia control (VIC) to suppress subsynchronous oscillation under the abnormal fluctuation of the operating point. Also, its structure ensures the reduction of calculation time while providing efficient damping and maintaining its nonlinear dynamic characteristics. Here, the simulation results were tested under the IEEE-39B system integrated with 2-WT. Furthermore, improved-PSO is intended to solve the problem of optimal power flow through a transmission line for a hybrid system by estimating output power using lognormal and weibull probability distribution functions (PDF) and lowering total generation cost, as proposed in [95].

The method of estimating the percentage of deloading for large-scale PV plants integrated in the transmission network using multiple linear regression analysis (MLRA) has been discussed in [96]. In this case, the simulation results are validated using a modified IEEE 39B test system. Also,

TABLE 3. An overview of the literature survey of WAPSS.

Reference	Design	System Dynamics	Technology	Remarks
Ref [69]	WADC	2A-4M	LST, LMI, SMRT	Improve CTD
Ref [70]	ATDC-WAPSS	2A-4M, 10M-39B NETS	Mixed H_2/H_∞ synthesis technique	Improve CTD
Ref [71]	WADC	2A-4M	LST, novel damping factor calculation	Improve damping factor
Ref [72]	WADC	MMPS	WAMS, GWO	Improve damping LFO, CTD, WAPSS parameter
Ref [73]	WADC	HILRT	Three different control algorithms are HILRT, dynamic output-feedback method, Bilinear transform method (BTM)	Improve damping LFO
Ref [74]	WAPSS	10M-39B NETS	JA, synchro-phasor measurements, TDC, geometric measures	Improve damping LFO, CTD, WAPSS parameter
Ref [75]	WADC	2A-4M, IEEE 5A-10M benchmark models	TDC, LST, PID compensator	Improve attenuation of noise pollution, damping LFO, CTD
Ref [76]	WADC	16M-68B	UR method, TDC	Improve damping LFO, WAPSS parameter, CTD
Ref [77]	WADC	IEEE 68B system	LMI method, PMU, polytopic model, AVR	Improve CTD, WAPSS parameter
Ref [78]	WAM-FO-PID controller	2A-benchmark system	PSO, ITAE, WAM-FO-PID, GDMRT	Improve DLFO, CTD, WAPSS parameter
Ref [79]	WAPSS	Single-area WAPS with Ethernet	DHMM- SP, EWMA	Improve damping LFO, CTD, WAPSS parameter
Ref [80]	WAPSS	16M-68B NETS	PMU, Transient energy function (TEF), Swarm intelligence-based techniques	Improve small-disturbance and transient angular stability problems
Ref [81]	WAPSS	IEEE 16M-68B NETS	Hybrid-PSO, PMU, polytopic modeling, LMI method	Improve damping LFO, CTD, WAPSS parameter

by comparing the proposed method with a battery energy storage system (BESS) and a synchronous condenser, which are installed in a PV integrated grid system, effectiveness is observed.

In [97], estimation method for optimal reactive power dispatch (ORPD) has been proposed for inclusion with the techniques of inheritance-non-dominated sorting genetic algorithm (i-NSGA-II) and roulette wheel selection to improve the performance of an integrated wind power system. The simulation results were validated using IEEE 33B and 69B test systems, as well as a modified Gilbert network.

A quantitative transient stability evaluation study framework was developed using a method of quantitatively estimating the influence of RES participation in power transmission lines on transient stability, as proposed in [98]. Table 4 summarises the literature review on renewable energy penetration.

VI. FACTS DEVICES WITH PSS COORDINATION AND THEIR CONTROL

CPSS is not able to damp both inter-area and intra-area oscillations simultaneously in an effective manner due to the limited observability of the system. PSS has a remarkable ability to effectively dampen power oscillations, whereas FACTS controllers are specifically intended to provide necessary reactive power, which eliminates the inter-area oscillations [99]. As a result, researchers are keen to develop advanced technology and controllers based on FACTS devices with PSS [99], [100]. Fig 9 depicts the block diagram of a two-area, four-machine 11-bus test system with a FACTS compensator [99].

In [99], a multi-input hierarchical FL PSS-based SVC (Static Var Compensator) has been designed for MMPS. Whereas, a hierarchical FL system has the quality of having a reduced number of rules as it consists of a number of low-dimensional FL systems in the form of a hierarchical structure. Here, SVC is the most efficient device for reactive power compensation, and its ability to provide a constant voltage supply has been proposed in [99]. Furthermore, as examined in [99], the multi-input hierarchical FL-PSS-based SVC performance outperforms CPSS, and the simulation results were tested on the 2A-4M-11B system.

In [100], WADC-based FACT devices (i.e., SVC) have been designed to damp inter-area oscillations in remote area signals where CTD is obtained from WAMS. Here, system feasibility is practically demonstrated and verified in a complex power system. Also, the simulation results were tested in 2A-4M power system, 10M-39B NETS, and 16M-68B power system. In [101] and [102], a decentralised Takagi Sugeno FL-WADC-based FACT controller is designed with the use of the probability collocation method for DFIG-WT to reduce the uncertainties from load parameters. Here, the simulation results were tested on a very large power system with 1332 buses and 39 buses of NETS.

A WADC-based STATCOM is designed in [103] to dampen the LFO by supplying appropriate auxiliary signals so that the generator rotor angle receives an appropriate signal to minimise speed deviation. A novel FL lead-lag

TABLE 4. An overview of the literature survey on renewable energy penetration.

Reference	Design	System Dynamics	Technology	Remarks
Ref [83]	Probabilistic-WAPSS-WT	2A system, IEEE-39B NETS	SMRT, DE algorithm	Improve damping LFO
Ref [84]	ESS-PSS for DFIG-WT	2A-4M, 10M-39B NETS	DTI, improved phase compensation method, flywheel storage technology, DFIG-WT	Improve damping LFO, TPP
Ref [85]	PSS for DFIG-WT	2A-4M	CPSO-passive congregation	Improve damping LFO, TPP
Ref [86]	Coordination of WAC-RES-Generators	10M-39B NETS	Prony analysis method, two-level hierarchical controller, EMT	Improve damping LFO
Ref [87]	WADC-photovoltaic integration	2A-4M, 16M-68B	LPV model, tensor product model, parallel distributed compensation controller, LMI, staircase basis function method	Improve CTD, parameter uncertain from photovoltaic generation
Ref [88]	WAPSS-WT	16M-68B	data transmission model, networked predictive control, online model identification, Gilbert model (GB)	Improve CTD, damping LFO, compensate dropouts packet data signals, parameter uncertain of DFIG
Ref [89]	PSS-WT	2A-11B	Type-II-FL, Multi objective-PSO, integral of square error method	Improve damping LFO, parameter uncertain from WT
Ref [90]	PODC-WT	16M-68B NETS	OODC, ROM, DFIG-WT, Balanced truncation method	Improve damping LFO, Enhancing system stability margin
Ref [91]	POD-DFIG	modified benchmark WSCC 9B	CKF, ADP, ARE, DSE, LQR, RPC	Improve damping LFO, Enhancing system stability margin
Ref [92]	WADC-FACTS-WT	8A-test system	ADC with synthesis H_∞/H_2 technique	Improve CTD, damping LFO
Ref [93]	Impact of power oscillation-FCT-WT	2A-4M	Investigation, inertia controller	Improvement in inertia response to damp oscillation
Ref [94]	Adaptive damping controller-Youla-Kucera-LPV-DFIG-WT	IEEE 39B system integrated with 2-WT	Supplementary damping controller, VIC, LPV, Youla-Kucera parameterization	Improve nonlinear dynamic characteristics (NDC), Computation time, parameter uncertain from WT
Ref [95]	Optimal power flow-Hybrid (WT-Solar)	Modified IEEE-30B with RES integration	Improved PSO, PDF	Reducing total generation cost, optimal power flow of Hybrid system
Ref [96]	Method for large-scale PV plants	Modified IEEE 39B test system	MLRA	Estimate deloading percentages of PV Plants
Ref [97]	Estimation solution of ORPD for wind integration system	IEEE 33B and 69B test system and modified real GB network	ORPD, genetic algorithm, roulette wheel selection method	Estimate optimal solution of ORPD for WT
Ref [98]	Method to calculate the effect renewable energy penetration	Modified IEEE 14B system	input-to-state stability theory	Calculated by quantitatively the effect renewable energy involvement

controller-based static synchronous series compensator has been designed to boost the stability of the power system [104]. In [105] and [106], the coordination of PSS and FACT devices with IPGSA and MTT has been proposed to improve the damping controller parameters, which optimize the damping ratio.

In [107], ACO-static synchronous compensator (STATCOM)-based voltage source converter is designed to damp a sub-synchronous LFO to improve the gain parameters of the controller. However, Fig 9 depicts a similar tested system block diagram [107].

In [108], a PSS-based GA and Grasshopper Optimization Algorithm (GOA) have been designed in order to optimize the parameters of the system. In [109] and [110], a PSS-based FACT device has been designed with a synchrosqueezed wavelet transform (SWT) and stochastic subspace identification (SSI) algorithm to deal with the LFO of a large-scale power system. Here, the controller parameters are to be optimized by the modified fruit fly optimization (FFO) algorithm as well as the Prony and UR methods.

To improve the damping performance of the LFO, [111] designed a PSS-based FFA and an IPFC as a supplementary

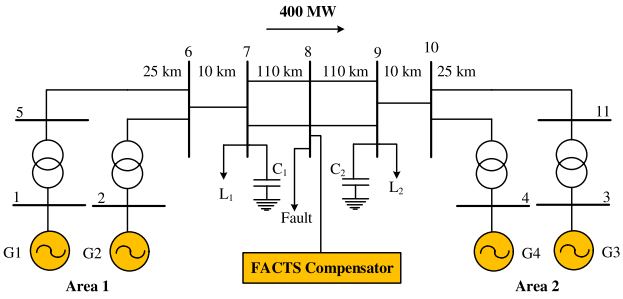

FIGURE 9. 2A-4M-11B test system with FACTS compensator.

controller. In [112], a PSS-based SVC with a UR-based approach has been designed to enhance the damping LFO. Here, the UR-based method is used to determine the optimal location of the proposed PSS. In order to optimise system performance, a FACTS device (SSSC) has been designed in collaboration with the POD controller as a supplementary controller [113].

In [114], WAPSS-based thyristor-controlled series capacitor (TCSC) has been designed for inter-area modes damping LFOs in addition to modal decomposition technique (MDM).

Here, the geometric measure of observability (GMO) provides the information of a feedback signal and improves the performance of the system. Whereas, the simulation of the system is evaluated in 2A-4M-11B with the integration of TCSC. Table 5 shows an overview of the literature survey of FACTS devices in coordination with PSS.

VII. ARTIFICIAL INTELLIGENCE AND FUZZY BASED PSS COORDINATION AND THEIR CONTROL

Nowadays, artificial intelligence (AI) is very popular due to the exponential increase in the strength of its prediction and forecasting [110]. [110] also demonstrated a PSS based on the farmland fertility algorithm (FFA) with interline power flow controllers (IPFC). Here, a neuro-fuzzy controller (NFC) has been developed as a damping controller to optimize the computational time. An artificial neural network (ANN) is trained by a large amount of data over a period of time, and then it can only predict the optimal parameters. But, still, neural networks are popular because they solve complex problems without any mathematical support [131].

In [115], an indirect adaptive FLPSS is designed to dampen inter-area oscillations. Here, PSO tunes the controller gain to ensure system stability and minimize the sum of the squares of speed variations. In [44], a single-input and dual-input PSS-based CASO algorithm is designed with the adoption of FL for very fast on-line, off-nominal feedback to improve the stabilizer parameters at various operating conditions.

In [116], a unique adaptive PSS based on both synergetic control and FL systems has been designed with LST to improve system stability. in addition to the adoption of a chatter-free continuous control rule, which simplifies the controller implementation. In [117], a PSS-based adaptive fuzzy sliding mode controller (AFSMC) has been designed to improve the transient dynamics and oscillation damping in a SMIB and MMPS.

Reference [118] developed a novel PSS-based AFSMC that employs Nussbaum gain on a nonlinear model subjected to a three-phase fault-enhancing damping LFO and transient dynamics. In [119], a PSS-based type-2 FL has been designed with a DE approach to optimize the system characteristics and rule. Here, the simulation results were tested in SMIB. A robust PSS-based indirect AFSMC has been designed that incorporates a PI controller and a sliding mode controller for damping local and inter-area oscillation modes for MMPS [120].

In [121], a hybrid strategy for tuning PSS in MMPS with an objective function to reduce LFO and enhance power system dynamic stability across a wide range of power systems has been proposed. In [122], a FL-PSS-based harmony search algorithm (HSA) has been designed to increase the input output scaling factors of the FL controller across a wide range of operating conditions. Here, the objective function for the optimization problem is the minimization of the integral square error. In addition, the performance indices of both systems (HSA and FL-PSS) have been examined.

Reference [124] designed an intelligent controller based on an AFSMC with a PI switching surface to minimise inter-area oscillations and damp the system's LFO. In [125], an adaptive FL-PSS has been designed by robust synergetic control theory and terminal attractor techniques to enhance damping LFO. Here, the performance of proposed stabilizers has been examined for SMIB and MMPS under various types of disturbances.

In [126], PSS-based conventional FL-PID and type-1-FL controller has been designed to improve the stability of SMIB and MMPS under various loading conditions. In [127], a FL-PSS-based krill herd algorithm (KHA) to dampen LFO has been proposed.

In [128], PSS-based FL controller has been designed to improve the performance of damping LFOs and tune the PSS parameters. Here, the advantage of this technique over conventional FL-PSS with constant parameters is that it optimizes the behaviour of a dynamic system. In [129], an AI-PID-PSS-based approach to an artificial bee colony (ABC) has been designed to minimize objective function by TPP and to provide suitable low-frequency mode damping. In [130], a PSS-based artificial immune system (AIS) has been designed to dampen LFO.

However, in order to successfully implement the framework of control design in power oscillations, numerous challenges of technology integration must be overcome. Table 6 shows an overview of the literature survey of artificial intelligence based PSS.

VIII. CURRENT ISSUES AND FUTURE CHALLENGES

Numerous research regarding the efficient design of PSSs have been reported. Several challenges have been observed in the development of PSSs. First, appropriate selection of controller parameters is a challenge since modern power systems are highly non-linear and uncertain. The suggested solution for the aforementioned problem is to design an advanced damping controller for modern power systems. Second, modeling of time-varying delay compensation and its consideration in design of wide-area power system stabilizers is one of the key challenges. Third, mitigating the effects of the penetration level of renewable energy sources and its coordination with existing PSS is a challenging task. The suggested solutions for the aforementioned problem are to optimize devices that facilitate the control of voltage fluctuations in grid and improve the variable renewable energy (VRE) forecasting technology. Fourth, fast continuous control of power flow in the transmission system by controlling voltages at critical buses is one of the key challenges for the application of FACTS damping controllers, which are coordinated with PSS for damping enhancement in the power system network. The suggested solution for the aforementioned problem is to develop advanced controller-based FACT devices to improve stability of the modern power systems. Further, a challenge with AI approaches is that they can only approximate future output if the training network is given ideal input and output. In addition, AI techniques require more computational

TABLE 5. An overview of the literature survey of FACTS devices in coordination with PSS.

Reference	Design	System Dynamics	Technology	Remarks
Ref [99]	SVC-PSS	2A-4M-11B	Hierarchical FL, Multi input PSS	Improve damping LFO
Ref [100]	WADC-FACTS(SVC)	2A-4M, 10M-39B NETS, 16M-68B	GMO, UR-method, LST criterion, LMI	Improve CTD
Ref [101]	WADC-FACT-DFIG-WT	10M-39B NETS developed on RTDS and on large practical Indian power system having 1332B	decentralized FL, robust H_∞ output feedback controller, probability collocation method, LMI, LST criterion, kalman filter, PMU	Reduced the uncertainties in load parameters, Improve damping LFO
Ref [102]	PODC for multipurpose	RTDS, 5A-16M-68B	STATCOM, SVC	Improve damping LFO
Ref [103]	WADC-FACTS	IEEE First Benchmark model	STATCOM	Improve damping oscillation in turbine-generator
Ref [104]	Coordinated FL lead lag structure-PSS-FACTS	MMPS	Modified WOA, SSSC controller, FL	Improve TPP
Ref [105]	PSS-FACTS	MMPS	IPGSA, MTT, BCC, PGSA, TCSC, Energy Storage, CSR	Improve damping LFO, TPP
Ref [106]	Comparative analysis of PSS, FACTS	SMIB	Investigation	Improve damping LFO, TPP
Ref [107]	FACTS controller	2A-4M-11B	ACO, STATCOM, PI controllers	Improve damping LFO, TPG, TPP
Ref [108]	Importance of GA GOA	SMIB	GA, GOA, SSSC controller	Improve damping LFO, TPP
Ref [109]	PSS-FACT-SWT, SSI	2A-4M, NETS 16M-68B	SWT, SSI, modified FFO algorithm, Prony UR-methods	Improve damping LFO, TPP
Ref [110]	PSS-IPFC-FFA	WSCC IEEE-3M system	FFA, IPFC, NFC, GA, PSO	Improve damping LFO, TPP, enhance computational cost, reduced number of parameters of the state feedback matrix
Ref [111]	PSS-IPFC-FFA	SMIB	IPFC, FFA	Improve damping LFO, TPP
Ref [112]	PSS-SVC	2A-4M-10B	SVC, UR-method	Improve damping LFO, optimal location of the SVC controller
Ref [113]	PSS-SSSC	IEEE-39B NETS	SSSC,UR-method	Improve damping LFO, TPP
Ref [114]	WAPSS-TCSC	2A-4M-11B	MDM, GMO	Improve damping LFO

TABLE 6. An overview of the literature survey on artificial intelligence based PSS.

Reference	Design	System Dynamics	Technology	Remarks
Ref [115]	PSS	2A-4M	AFSMC, PSO	Improve DLFO, TPG
Ref [44]	PSS	SMIB	TSFL, CASO algorithms, AVR	Improve TPP
Ref [116]	PSS	SMIB	LS, AFSMC, PSO algorithm	Improve DLFO, TPP
Ref [117]	PSS	SMIB	AFSMC	Improve DLFO
Ref [118]	PSS	SMIB, MMPS	AFSMC, Nussbaum gain	Improve DLFO
Ref [119]	PSS	SMIB, MMPS	type-2 FL, DE algorithm	Improve DLFO, TPP
Ref [120]	PSS	2A-4M	AFSMC, PI controller	Improve DLFO
Ref [121]	PSS	2A-4M	PSO algorithm, TSFL	Improve DLFO, TPP
Ref [122]	PSS	2A-4M	HSA, FL	Improve input-output scaling factors, DLFO, TPP
Ref [123]	PSS	SMIB	FL-PSS, PID controller, and PSO-based PID controller	Improve DLFO
Ref [124]	PSS	2A-4M	AFSMC, PI	Improve DLFO
Ref [125]	PSS	SMIB, MMPS	AFSMC	Improve DLFO
Ref [126]	PSS	OPAL-RT-OP5600	Conventional FL-PID and type-1-FL controller, AFSMC	Improve DLFO
Ref [127]	PSS	16M-68B	KHA, cascaded-FL, conventional IEEE linear lead-lag PSS	Improve DLFO, TPP
Ref [128]	PID-PSS-AI	3M-9B	PID, PSO	Improve DLFO, TPP
Ref [129]	Hybrid PID-PSS	3M-9B	Hybrid PID, ABC	Improve DLFO, TPP
Ref [130]	PSS	4M-10B	AIS	Improve DLFO

time to predict the outcome, which is one of the challenges. The suggested solution for the aforementioned problem is to develop some hybrid AI-based technique so that the prediction capability of AI becomes more accurate.

IX. CONCLUSION

Modern day power systems are structurally complex. It is highly susceptible to transient events like faults and outages, which may eventually lead to the instability of the system. Therefore, secure and reliable operation of the power system is highly desirable. Rotor angle instability is one such instability that may disrupt a secure and reliable power supply. Consequently, the problem of rotor angle instability must be tackled efficiently. PSSs are devices that are capable of damping power oscillations in the systems, thereby reducing the impact of rotor angle instabilities. However, designing a

robust and efficient PSS is currently a difficult task. Several techniques are reported in the literature for the design of PSSs. However, the increase in complexities in modern power systems compels more efficient designs of PSSs that can tackle modern day uncertainties. In the present study, techniques developed to design PSSs are categorically discussed, and future challenges are highlighted.

REFERENCES

[1] P. Kundur, N. J. Balu, and M. G. Lauby, *Power System Stability and Control*, vol. 7. New York, NY, USA: McGraw-Hill, 1994.

[2] P. Kundur, "Power system stability," in *Power System Stability and Control*, vol. 10. Boca Raton, FL, USA: CRC Press, 2007.

[3] K. R. Padiyar, *Power System Dynamics: Stability and Control*. New York, NY, USA: Wiley, 1996.

[4] P. W. Sauer, M. A. Pai, and J. H. Chow, *Power System Dynamics and Stability: With Synchrophasor Measurement and Power System Toolbox*. Hoboken, NJ, USA: Wiley, 2017.

[5] M. A. Ibrahim, *Disturbance Analysis for Power Systems*. Hoboken, NJ, USA: Wiley, 2011.

[6] M. Aien, A. Hajebrahimi, and M. Fotuhi-Firuzabad, "A comprehensive review on uncertainty modeling techniques in power system studies," *Renew. Sustain. Energy Rev.*, vol. 57, pp. 1077–1089, May 2016.

[7] H. Haes Alhelou, M. E. Hamedani-Golshan, T. C. Njenda, and P. Siano, "A survey on power system blackout and cascading events: Research motivations and challenges," *Energies*, vol. 12, no. 4, p. 682, 2019.

[8] The New Indian Express. (2021). *Sri Lankan Police Launch Probe in Major Power Outage*. Accessed: Dec. 3, 2021. [Online]. Available: https://www.newindianexpress.com/world/2021/dec/03/sri-lankan-police-launch-probe-in-major-power-outage-2391417.html

[9] The National News. (2021). *Jordan Hit by Widespread Power Cut*. Accessed: May 21, 2021. [Online]. Available: https://www.thenationalnews.com/mena/jordan/jordan-hit-by-widespread-power-cut-1.1227062

[10] The NYPS Times. (2021). *Much of Pakistan Loses Power in Massive Blackout*. Accessed: Jan. 9, 2021. [Online]. Available: https://www.nytimes.com/2021/01/09/world/asia/pakistan-blackout-power-failure.html

[11] An Echelon Media Company. (2020). *Sri Lanka Power Blackout as Grid Hit by Cascading Failure*. Accessed: Dec. 3, 2021. [Online]. Available: https://economynext.com/sri-lanka-power-blackout-as-grid-hit-by-cascading-failure-88442/

[12] A. B. D. Costa and G. Suroyo. (2019). Power restored to some areas in Indonesia capital, parts of Java after 9 hours. Reuters. Accessed: Aug. 4, 2019. [Online]. Available: https://www.reuters.com/article/us-indonesia-power-idUSKCN1UU060

[13] AP News. (2019). *Indonesian Capital Hit by Massive 8-Hour Power Outage*. Accessed: Aug. 4, 2019. [Online]. Available: https://t.ly/1Hli9

[14] S. Pozzebon and B. Britton. (2019). *Huge Power Outage Leaves Most of Venezuela in Darkness*. Accessed: Mar. 9, 2019. [Online]. Available: https://edition.cnn.com/2019/03/08/americas/venezuela-blackout-power-intl/index.html

[15] V. Sequera and D. Buitrago. (2019). Venezuela, blaming U.S. for six-day blackout, orders diplomats to leave. REUTERS. Accessed: Mar. 12, 2019. [Online]. Available: https://t.ly/jIUU

[16] M. F. Ali, and A. R. Pananrang. (2018). *Apa ITU Black Out? Ini Penyebab Listrik Sulsel Padam, Kapan Pemadaman Berakhir?* Accessed: Nov. 15, 2018. [Online]. Available: https://t.ly/fJhf

[17] L. Costa and L. Goy. (2018). Tens of millions in northern Brazil hit by massive power outage. REUTERS. Accessed: Mar. 21, 2018. [Online]. Available: https://www.reuters.com/article/us-brazil-power-idUSKBN1GX3CN

[18] The NDTV. (2016). *Sri Lanka Faces Nationwide Power Blackout; Water Supply Affected*. Accessed: Mar. 13, 2016. [Online]. Available: https://t.ly/XNQ9

[19] The Guardian and World News. (2015). *Massive Power Failure Plunges 80% of Pakistan Into Darkness*. Accessed: Jan. 25, 2015. [Online]. Available: https://www.theguardian.com/world/2015/jan/25/massive-power-failure-plunges-80-of-pakistan-into-darkness

[20] S. Z. Al-Mahmood. (2014). *Bangladesh Power Restored After Nationwide Blackout*. Accessed: Nov. 2, 2014. [Online]. Available: https://www.wsj.com/articles/bangladesh-power-restored-after-nationwide-blackout-1414915894

[21] Helen Pidd. (2012). India blackouts leave 700 million without power. The Guardian. Accessed: Jul. 31, 2012. [Online]. Available: https://www.theguardian.com/world/2012/jul/31/india-blackout-electricity-power-cuts

[22] M. A. Hannan, N. N. Islam, A. Mohamed, M. S. H. Lipu, P. J. Ker, M. M. Rashid, and H. Shareef, "Artificial intelligent based damping controller optimization for the multi-machine power system: A review," *IEEE Access*, vol. 6, pp. 39574–39594, 2018.

[23] R. Devarapalli, N. K. Sinha, and F. P. G. Márquez, "A review on the computational methods of power system stabilizer for damping power network oscillations," *Arch. Comput. Methods Eng.*, vol. 29, pp. 3713–3739, Feb. 2022.

[24] Z. Rafique, H. M. Khalid, S. Muyeen, and I. Kamwa, "Bibliographic review on power system oscillations damping: An era of conventional grids and renewable energy integration," *Int. J. Electr. Power Energy Syst.*, vol. 136, Mar. 2022, Art. no. 107556.

[25] Y. Tang, F. Li, Q. Wang, and Y. Xu, "Hybrid method for power system transient stability prediction based on two-stage computing resources," *IET Gener., Transmiss. Distrib.*, vol. 12, no. 8, pp. 1697–1703, Apr. 2018.

[26] L. L. Grigsby, *Power System Stability and Control*. Boca Raton, FL, USA: CRC Press, 2007.

[27] M. Pai, D. S. Gupta, and K. Padiyar, *Small Signal Analysis of Power Systems*. London, U.K.: Alpha Science International, 2004.

[28] H. U. Banna, A. Luna, P. Rodriguez, A. Cabrera, H. Ghorbani, and S. Ying, "Performance analysis of conventional PSS and fuzzy controller for damping power system oscillations," in *Proc. Int. Conf. Renew. Energy Res. Appl. (ICRERA)*, Oct. 2014, pp. 229–234.

[29] B. Shah, "Comparative study of conventional and fuzzy based power system stabilizer," in *Proc. Int. Conf. Commun. Syst. Netw. Technol.*, 2013, pp. 547–551.

[30] M. Soliman, A. L. Elshafei, F. Bendary, and W. Mansour, "Robust decentralized PID-based power system stabilizer design using an ILMI approach," *Electr. Power Syst. Res.*, vol. 80, no. 12, pp. 1488–1497, Dec. 2010.

[31] Y. Peng, Q. M. Zhu, and H. Nouri, "Robust H_2 power system stabilizer design using LMI techniques," in *Proc. Int. Conf. Modelling, Identificat. Control*, 2011, pp. 405–410.

[32] J. Ma, H. Wang, and P. Zhang, "Renewed investigation on power system stabilizer design," *Sci. China Technol. Sci.*, vol. 54, no. 10, pp. 2687–2693, Oct. 2011.

[33] D. Sumina, N. Bulić, and M. Mišković, "Parameter tuning of power system stabilizer using eigenvalue sensitivity," *Electric Power Syst. Res.*, vol. 81, no. 12, pp. 2171–2177, Dec. 2011.

[34] A. Horch, A. Naceri, and A. Ayad, "Power system stabilizer design using H_∞ robust technique to enhance robustnesse of power system," in *Proc. Int. Renew. Sustain. Energy Conf. (IRSEC)*, Oct. 2014, pp. 884–889.

[35] S. Santra and S. Paul, "PSO based robust power system stabilizer design using mixed sensitivity based h output-feedback control in LMI approach," in *Proc. 3rd Int. Conf. Res. Comput. Intell. Commun. Netw. (ICRCICN)*, Nov. 2017, pp. 273–278.

[36] A. Salgotra and S. Pan, "Model based PI power system stabilizer design for damping low frequency oscillations in power systems," *ISA Trans.*, vol. 76, pp. 110–121, May 2018.

[37] A. Yakout, W. Sabry, and H. M. Hasanien, "Enhancing rotor angle stability of power systems using marine predator algorithm based cascaded PID control," *Ain Shams Eng. J.*, vol. 12, no. 2, pp. 1849–1857, Jun. 2021.

[38] A. F. Rashwan, M. Ahmed, M. R. Mossa, A. M. Baha-El-Din, S. Alkhalaf, T. Senjyu, and A. M. Hemeida, "Explicit adaptive power system stabilizer design based an on-line identifier for single-machine infinite bus," *Ain Shams Eng. J.*, vol. 13, no. 2, Mar. 2022, Art. no. 101544.

[39] R. A. Jabr, B. C. Pal, and N. Martins, "A sequential conic programming approach for the coordinated and robust design of power system stabilizers," *IEEE Trans. Power Syst.*, vol. 25, no. 3, pp. 1627–1637, Aug. 2010.

[40] E. Babaei and V. Hosseinnezhad, "A QPSO based parameters tuning of the conventional power system stabilizer," in *Proc. Conf. Proc. IPEC*, Oct. 2010, pp. 467–471.

[41] Z. Wang, C. Y. Chung, K. P. Wong, D. Gan, and Y. Xue, "Probabilistic power system stabilizer design with consideration of optimal siting using recursive genetic algorithm," *Eur. Trans. Electr. Power*, vol. 21, no. 3, pp. 1409–1424, Apr. 2011.

[42] M. O. Hassan, S. J. Cheng, and Z. A. Zakaria, "Optimization of conventional power system stabilizer to improve dynamic stability," in *Proc. 5th IEEE Conf. Ind. Electron. Appl.*, Jun. 2010, pp. 599–604.

[43] M. Eslami, H. Shareef, and A. Mohamed, "Power system stabilizer design using hybrid multi-objective particle swarm optimization with chaos," *J. Central South Univ.*, vol. 18, no. 5, pp. 1579–1588, Oct. 2011.

[44] A. Chatterjee, S. P. Ghoshal, and V. Mukherjee, "Chaotic ant swarm optimization for fuzzy-based tuning of power system stabilizer," *Int. J. Electr. Power Energy Syst.*, vol. 33, no. 3, pp. 657–672, Mar. 2011.

[45] A. Stativă, M. Gavrilaş, and V. Stahie, "Optimal tuning and placement of power system stabilizer using particle swarm optimization algorithm," in *Proc. Int. Conf. Expo. Electr. Power Eng.*, Oct. 2012, pp. 242–247.

[46] A. Khodabakhshian and R. Hemmati, "Multi-machine power system stabilizer design by using cultural algorithms," *Int. J. Electr. Power Energy Syst.*, vol. 44, no. 1, pp. 571–580, Jan. 2013.

[47] A. Khodabakhshian, R. Hemmati, and M. Moazzami, "Multi-band power system stabilizer design by using CPCE algorithm for multi-machine power system," *Electr. Power Syst. Res.*, vol. 101, pp. 36–48, Aug. 2013.

[48] D. K. Sambariya and R. Prasad, "Robust tuning of power system stabilizer for small signal stability enhancement using metaheuristic bat algorithm," *Int. J. Electr. Power Energy Syst.*, vol. 61, pp. 229–238, Oct. 2014.

[49] R. Sheeba, M. Jayaraju, and K. Sundareswaran, "Performance enhancement of power system stabilizer through colony of foraging ants," *Electr. Power Compon. Syst.*, vol. 42, no. 10, pp. 1016–1028, Jul. 2014.

[50] M. Mohammadi and N. Ghadimi, "Optimal location and optimized parameters for robust power system stabilizer using honeybee mating optimization," *Complexity*, vol. 21, no. 1, pp. 242–258, Sep. 2015.

[51] D. Chitara, A. Swarnkar, N. Gupta, K. R. Niazi, and R. C. Bansal, "Optimal tuning of multimachine power system stabilizer using cuckoo search algorithm," *IFAC-PapersOnLine*, vol. 48, no. 30, pp. 143–148, 2015.

[52] D. K. Sambariya and R. Prasad, "Design of optimal proportional integral derivative based power system stabilizer using bat algorithm," *Appl. Comput. Intell. Soft Comput.*, vol. 2016, pp. 1–22, Mar. 2016.

[53] S. M. A. Elazim and E. S. Ali, "Optimal power system stabilizers design via cuckoo search algorithm," *Int. J. Electr. Power Energy Syst.*, vol. 75, pp. 99–107, Feb. 2016.

[54] P. Jagadeesh and M. S. Veerraju, "Particle swarm optimization based power system stabilizer for SMIB system," in *Proc. Int. Conf. Emerg. Trends Eng., Technol. Sci. (ICETETS)*, Feb. 2016, pp. 1–6.

[55] P. K. Ray, S. R. Paital, A. Mohanty, T. K. Panigrahi, M. Kumar, and H. Dubey, "Swarm and bacterial foraging based optimal power system stabilizer for stability improvement," in *Proc. IEEE Region 10 Conf. (TENCON)*, Nov. 2016, pp. 1916–1920.

[56] L. Chaib, A. Choucha, and S. Arif, "Optimal design and tuning of novel fractional order PID power system stabilizer using a new metaheuristic bat algorithm," *Ain Shams Eng. J.*, vol. 8, no. 2, pp. 113–125, Jun. 2017.

[57] D. Wang, N. Ma, M. Wei, and Y. Liu, "Parameters tuning of power system stabilizer PSS4B using hybrid particle swarm optimization algorithm," *Int. Trans. Electr. Energy Syst.*, vol. 28, no. 9, p. e2598, Sep. 2018.

[58] D. Chitara, K. R. Niazi, A. Swarnkar, and N. Gupta, "Cuckoo search optimization algorithm for designing of a multimachine power system stabilizer," *IEEE Trans. Ind. Appl.*, vol. 54, no. 4, pp. 3056–3065, Jul./Aug. 2018.

[59] P. R. Sahu, P. K. Hota, and S. Panda, "Power system stability enhancement by fractional order multi input SSSC based controller employing whale optimization algorithm," *J. Elect. Syst. Inf. Technol.*, vol. 5, no. 3, pp. 326–336, Dec. 2018.

[60] B. Dasu, M. S. Kumar, and R. S. Rao, "Design of robust modified power system stabilizer for dynamic stability improvement using particle swarm optimization technique," *Ain Shams Eng. J.*, vol. 10, no. 4, pp. 769–783, Dec. 2019.

[61] B. Dasu, M. Sivakumar, and R. Srinivasarao, "Interconnected multimachine power system stabilizer design using whale optimization algorithm," *Protection Control Mod. Power Syst.*, vol. 4, no. 1, pp. 1–11, Dec. 2019.

[62] M. Rahmatian and S. Seyedtabaii, "Multi-machine optimal power system stabilizers design based on system stability and nonlinearity indices using hyper-spherical search method," *Int. J. Electr. Power Energy Syst.*, vol. 105, pp. 729–740, Feb. 2019.

[63] D. Butti, S. K. Mangipudi, and S. R. Rayapudi, "An improved whale optimization algorithm for the design of multi-machine power system stabilizer," *Int. Trans. Electr. Energy Syst.*, vol. 30, no. 5, May 2020, Art. no. e12314.

[64] D. Izci, "A novel improved atom search optimization algorithm for designing power system stabilizer," *Evol. Intell.*, vol. 15, pp. 2089–2103, May 2021.

[65] R. Devarapalli, B. Bhattacharyya, N. K. Sinha, and B. Dey, "Amended GWO approach based multi-machine power system stability enhancement," *ISA Trans.*, vol. 109, pp. 152–174, Mar. 2021.

[66] B. S. Surjan and R. Garg, "Power system stabilizer controller design for SMIB stability study," *Int. J. Eng. Adv. Technol.*, vol. 2, no. 1, pp. 209–214, 2012.

[67] S. K. Wang, "A novel objective function and algorithm for optimal PSS parameter design in a multi-machine power system," *IEEE Trans. Power Syst.*, vol. 28, no. 1, pp. 522–531, Feb. 2013.

[68] A. M. Gajarea and R. Singhb, "Performance analysis of GWO GA and PSO optimized FOPID and PSS for SMIB system," *Int. J. Control Theory Appl.*, vol. 10, no. 35, pp. 239–262, 2017.

[69] W. Yao, L. Jiang, Q. H. Wu, J. Y. Wen, and S. J. Cheng, "Delay-dependent stability analysis of the power system with a wide-area damping controller embedded," *IEEE Trans. Power Syst.*, vol. 26, no. 1, pp. 233–240, Feb. 2011.

[70] M. Beiraghi and A. M. Ranjbar, "Adaptive delay compensator for the robust wide-area damping controller design," *IEEE Trans. Power Syst.*, vol. 31, no. 6, pp. 4966–4976, Nov. 2016.

[71] B. Yang and Y. Sun, "A novel approach to calculate damping factor based delay margin for wide area damping control," *IEEE Trans. Power Syst.*, vol. 29, no. 6, pp. 3116–3117, Nov. 2014.

[72] M. R. Shakarami and I. F. Davoudkhani, "Wide-area power system stabilizer design based on grey wolf optimization algorithm considering the time delay," *Elect. Power Syst. Res.*, vol. 133, pp. 149–159, Apr. 2016.

[73] Y. Li, Y. Zhou, F. Liu, Y. Cao, and C. Rehtanz, "Design and implementation of delay-dependent wide-area damping control for stability enhancement of power systems," *IEEE Trans. Smart Grid*, vol. 8, no. 4, pp. 1831–1842, Jul. 2017.

[74] T. Prakash, V. P. Singh, and S. R. Mohanty, "A synchrophasor measurement based wide-area power system stabilizer design for inter-area oscillation damping considering variable time-delays," *Int. J. Electr. Power Energy Syst.*, vol. 105, pp. 131–141, Feb. 2019.

[75] S. Roy, A. Patel, and I. N. Kar, "Analysis and design of a wide-area damping controller for inter-area oscillation with artificially induced time delay," *IEEE Trans. Smart Grid*, vol. 10, no. 4, pp. 3654–3663, Jul. 2019.

[76] J. Qi, Q. Wu, Y. Zhang, G. Weng, and D. Zhou, "Unified residue method for design of compact wide-area damping controller based on power system stabilizer," *J. Modern Power Syst. Clean Energy*, vol. 8, no. 2, pp. 367–376, 2020.

[77] M. E. C. Bento and R. A. Ramos, "A method based on linear matrix inequalities to design a wide-area damping controller resilient to permanent communication failures," *IEEE Syst. J.*, vol. 15, no. 3, pp. 3832–3840, Sep. 2021.

[78] M. Saadatmand, B. Mozafari, G. B. Gharehpetian, and S. Soleymani, "Optimal coordinated tuning of power system stabilizers and wide-area measurement-based fractional-order PID controller of large-scale PV farms for LFO damping in smart grids," *Int. Trans. Electr. Energy Syst.*, vol. 31, no. 2, 2021, Art. no. e12612.

[79] H. Mo and G. Sansavini, "Hidden Markov model-based Smith predictor for the mitigation of the impact of communication delays in wide-area power systems," *Appl. Math. Model.*, vol. 89, pp. 19–48, Jan. 2021.

[80] R. N. D. Costa Filho and V. L. Paucar, "A multi-objective optimization model for robust tuning of wide-area PSSs for enhancement and control of power system angular stability," *Results Control Optim.*, vol. 3, Jun. 2021, Art. no. 100011.

[81] M. E. C. Bento, "A hybrid particle swarm optimization algorithm for the wide-area damping control design," *IEEE Trans. Ind. Informat.*, vol. 18, no. 1, pp. 592–599, Jan. 2022.

[82] H. Terfa, L. Baghli, and R. Bhandari, "Impact of renewable energy micropower plants on power grids over Africa," *Energy*, vol. 238, Jan. 2022, Art. no. 121702.

[83] D. Ke and C. Y. Chung, "Design of probabilistically-robust wide-area power system stabilizers to suppress inter-area oscillations of wind integrated power systems," *IEEE Trans. Power Syst.*, vol. 31, no. 6, pp. 4297–4309, Nov. 2016.

[84] L. Shi, K. Y. Lee, and F. Wu, "Robust ESS-based stabilizer design for damping inter-area oscillations in multimachine power systems," *IEEE Trans. Power Syst.*, vol. 31, no. 2, pp. 1395–1406, Mar. 2016.

[85] M. Derafshian and N. Amjady, "Optimal design of power system stabilizer for power systems including doubly fed induction generator wind turbines," *Energy*, vol. 84, pp. 1–14, May 2015.

[86] L. Zacharia, L. Hadjidemetriou, and E. Kyriakides, "Integration of renewables into the wide area control scheme for damping power oscillations," *IEEE Trans. Power Syst.*, vol. 33, no. 5, pp. 5778–5786, Sep. 2018.

[87] Y. Zhou, J. Liu, Y. Li, C. Gan, H. Li, and Y. Liu, "A gain scheduling wide-area damping controller for the efficient integration of photovoltaic plant," *IEEE Trans. Power Syst.*, vol. 34, no. 3, pp. 1703–1715, May 2019.

[88] J. Nan, W. Yao, J. Wen, Y. Peng, J. Fang, X. Ai, and J. Wen, "Wide-area power oscillation damper for DFIG-based wind farm with communication delay and packet dropout compensation," *Int. J. Electr. Power Energy Syst.*, vol. 124, Jan. 2021, Art. no. 106306.

[89] P. R. Nakhi and M. A. Kamarposhti, "Multi objective design of type II fuzzy based power system stabilizer for power system with wind farm turbine considering uncertainty," *Int. Trans. Electr. Energy Syst.*, vol. 30, no. 4, Apr. 2020, Art. no. e12285.

[90] N. Gurung, R. Bhattarai, and S. Kamalasadan, "Optimal oscillation damping controller design for large-scale wind integrated power grid," *IEEE Trans. Ind. Appl.*, vol. 56, no. 4, pp. 4225–4235, Jul./Aug. 2020.

[91] A. S. Mir and N. Senroy, "DFIG damping controller design using robust CKF-based adaptive dynamic programming," *IEEE Trans. Sustain. Energy*, vol. 11, no. 2, pp. 839–850, Apr. 2020.

[92] M. Darabian and A. Bagheri, "Design of adaptive wide-area damping controller based on delay scheduling for improving small-signal oscillations," *Int. J. Electr. Power Energy Syst.*, vol. 133, Dec. 2021, Art. no. 107224.

[93] M. Edrah, X. Zhao, W. Hung, P. Qi, B. Marshall, S. Baloch, and A. Karcanias, "Electromechanical interactions of full scale converter wind turbine with power oscillation damping and inertia control," *Int. J. Electr. Power Energy Syst.*, vol. 135, Feb. 2022, Art. no. 107522.

[94] T. Wang, M. Jin, Y. Li, J. Wang, Z. Wang, and S. Huang, "Adaptive damping control scheme for wind grid-connected power systems with virtual inertia control," *IEEE Trans. Power Syst.*, vol. 37, no. 5, pp. 3902–3912, Sep. 2022.

[95] M. K. Ahmed, M. H. Osman, and N. V. Korovkin, "OPF solution based on improved PSO algorithm considering stochastic solar and wind power," in *Proc. Int. Conf. Electrotech. Complexes Syst. (ICOECS)*, Nov. 2021, pp. 549–554.

[96] A. Jawad and N. A. Masood, "A systematic approach to estimate the frequency support from large-scale PV plants in a renewable integrated grid," *Energy Rep.*, vol. 8, pp. 940–954, Nov. 2022.

[97] Y. Liu, D. Ćetenović, H. Li, E. Gryazina, and V. Terzija, "An optimized multi-objective reactive power dispatch strategy based on improved genetic algorithm for wind power integrated systems," *Int. J. Electr. Power Energy Syst.*, vol. 136, Mar. 2022, Art. no. 107764.

[98] S. Niu, Z. Zhang, X. Ke, G. Zhang, C. Huo, and B. Qin, "Impact of renewable energy penetration rate on power system transient voltage stability," *Energy Rep.*, vol. 8, pp. 487–492, Apr. 2022.

[99] M. H. Raouf, E. R. Anarmarzi, H. Lesani, and J. Olamaei, "Power system damping using hierarchical fuzzy multi-input power system stabilizer and static VAR compensator," *Int. J. Electr. Electron. Eng.*, vol. 5, no. 2, pp. 117–123, 2011.

[100] W. Yao, L. Jiang, J. Wen, Q. H. Wu, and S. Cheng, "Wide-area damping controller of FACTS devices for inter-area oscillations considering communication time delays," *IEEE Trans. Power Syst.*, vol. 29, no. 1, pp. 318–329, Jan. 2014.

[101] V. V. G. Krishnan, S. Srivastava, and S. Chakrabarti, "A robust decentralized wide area damping controller for wind generators and FACTS controllers considering load model uncertainties," *IEEE Trans. Smart Grid*, vol. 9, no. 1, pp. 360–372, Jan. 2018.

[102] C. Li, J. Deng, and X.-P. Zhang, "Coordinated design and application of robust damping controllers for shunt FACTS devices to enhance small-signal stability of large-scale power systems," *CSEE J. Power Energy Syst.*, vol. 3, no. 4, pp. 399–407, Dec. 2017.

[103] R. Giri, V. Jain, and A. Kumar, "Analysis and design of wide area damping controller for STATCOM in series compensated power system," in *Proc. Int. Conf. Smart City Emerg. Technol. (ICSCET)*, Jan. 2018, pp. 1–10.

[104] P. R. Sahu, P. K. Hota, and S. Panda, "Modified whale optimization algorithm for coordinated design of fuzzy lead-lag structure-based SSSC controller and power system stabilizer," *Int. Trans. Electr. Energy Syst.*, vol. 29, no. 4, Apr. 2019, Art. no. e2797.

[105] G. Yu, T. Lin, J. Zhang, Y. Tian, and X. Yang, "Coordination of PSS and FACTS damping controllers to improve small signal stability of large-scale power systems," *CSEE J. Power Energy Syst.*, vol. 5, no. 4, pp. 507–514, Dec. 2019.

[106] K. Kumar, S. K. Parida, and P. Kumar Biswas, "Comparative analysis of PSS and IPFC based damping controller for SMIB system," in *Proc. 8th Int. Conf. Power Syst. (ICPS)*, Dec. 2019, pp. 1–6.

[107] R. Kumar, R. Singh, and H. Ashfaq, "Stability enhancement of multi-machine power systems using ant colony optimization-based static synchronous compensator," *Comput. Electr. Eng.*, vol. 83, May 2020, Art. no. 106589.

[108] S. Ralhan, M. Patil, M. Singh, and D. K. Verma, "Damping of power system oscillations using GA and GOA optimized SSSC based controller," in *Proc. 1st Int. Conf. Power, Control Comput. Technol. (ICPC2T)*, Jan. 2020, pp. 277–282.

[109] A. Faraji, A. H. Naghshbandy, and A. G. Baayeh, "A hybrid coordinated design method for power system stabilizer and FACTS device based on synchrosqueezed wavelet transform and stochastic subspace identification," *J. Mod. Power Syst. Clean Energy*, vol. 9, no. 4, pp. 910–918, 2021.

[110] A. Sabo, N. I. A. Wahab, M. L. Othman, M. Z. A. B. M. Jaffar, H. Acikgoz, H. Nafisi, and H. Shahinzadeh, "Artificial intelligence-based power system stabilizers for frequency stability enhancement in multi-machine power systems," *IEEE Access*, vol. 9, pp. 166095–166116, 2021.

[111] A. Sabo, N. I. A. Wahab, and M. L. Othman, "Coordinated design of PSS and IPFC using FFA to control low frequency oscillations," in *Proc. IEEE 19th Student Conf. Res. Develop. (SCOReD)*, Nov. 2021, pp. 201–206.

[112] C. V. Rohit, K. Yadav, and P. B. Darji, "Optimal placement of SVC using residue technique and coordination with PSS for damping inter-area oscillations," in *Proc. 31st Australas. Univ. Power Eng. Conf. (AUPEC)*, Sep. 2021, pp. 1–6.

[113] C. E. Pupin, E. V. Fortes, P. B. de Araujo, and L. H. Macedo, "Power flow control and small-signal stability analysis considering the SSSC FACTS," in *Proc. 14th IEEE Int. Conf. Ind. Appl. (INDUSCON)*, Aug. 2021, pp. 15–22.

[114] A. Prakash, P. Singh, K. Kumar, and S. K. Parida, "Design of TCSC based optimal wide area power system stabilizer for low-frequency oscillation," in *Proc. IEEE 4th Int. Conf. Comput., Power Commun. Technol. (GUCON)*, Sep. 2021, pp. 1–6.

[115] T. Hussein, M. S. Saad, A. L. Elshafei, and A. Bahgat, "Damping inter-area modes of oscillation using an adaptive fuzzy power system stabilizer," *Electr. Power Syst. Res.*, vol. 80, no. 12, pp. 1428–1436, Dec. 2010.

[116] Z. Bouchama and M. N. Harmas, "Optimal robust adaptive fuzzy synergetic power system stabilizer design," *Electr. Power Syst. Res.*, vol. 83, no. 1, pp. 170–175, Feb. 2012.

[117] E. Nechadi, M. N. Harmas, A. Hamzaoui, and N. Essounbouli, "A new robust adaptive fuzzy sliding mode power system stabilizer," *Int. J. Electr. Power Energy Syst.*, vol. 42, no. 1, pp. 1–7, Nov. 2012.

[118] E. Nechadi, M. N. Harmas, N. Essounbouli, and A. Hamzaoui, "Adaptive fuzzy sliding mode power system stabilizer using Nussbaum gain," *Int. J. Autom. Comput.*, vol. 10, no. 4, pp. 281–287, Aug. 2013.

[119] Z. Sun, N. Wang, D. Srinivasan, and Y. Bi, "Optimal tunning of type-2 fuzzy logic power system stabilizer based on differential evolution algorithm," *Int. J. Elect. Power Energy Syst.*, vol. 62, no. 11, pp. 19–28, 2014.

[120] K. Saoudi and M. N. Harmas, "Enhanced design of an indirect adaptive fuzzy sliding mode power system stabilizer for multi-machine power systems," *Int. J. Electr. Power Energy Syst.*, vol. 54, pp. 425–431, Jan. 2014.

[121] V. Keumarsi, M. Simab, and G. Shahgholian, "An integrated approach for optimal placement and tuning of power system stabilizer in multi-machine systems," *Int. J. Electr. Power Energy Syst.*, vol. 63, pp. 132–139, Dec. 2014.

[122] D. K. Sambariya and R. Prasad, "Optimal tuning of fuzzy logic power system stabilizer using harmony search algorithm," *Int. J. Fuzzy Syst.*, vol. 17, no. 3, pp. 457–470, Sep. 2015.

[123] S. Paliwal, P. Sharma, and A. K. Sharma, "Dynamic stability enhancement of power system using intelligent power system stabilizer," in *Proc. 4th Int. Conf. Soft Comput. Problem Solving*. India: Springer, 2015, pp. 571–583.
[124] M. Farahani and S. Ganjefar, "Intelligent power system stabilizer design using adaptive fuzzy sliding mode controller," *Neurocomputing*, vol. 226, pp. 135–144, Feb. 2017.
[125] Z. Bouchama, N. Essounbouli, M. N. Harmas, A. Hamzaoui, and K. Saoudi, "Reaching phase free adaptive fuzzy synergetic power system stabilizer," *Int. J. Electr. Power Energy Syst.*, vol. 77, pp. 43–49, May 2016.
[126] P. K. Ray, S. R. Paital, A. Mohanty, F. Y. S. Eddy, and H. B. Gooi, "A robust power system stabilizer for enhancement of stability in power system using adaptive fuzzy sliding mode control," *Appl. Soft Comput.*, vol. 73, pp. 471–481, Dec. 2018.
[127] B. Douidi, L. Mokrani, and M. Machmoum, "A new cascade fuzzy power system stabilizer for multi-machine system stability enhancement," *J. Control, Autom. Electr. Syst.*, vol. 30, no. 5, pp. 765–779, Oct. 2019.
[128] A. Jalilvand, R. Aghmasheh, and E. Khalkhali, "Robust design of PID power system stabilizer in multi-machine power system using artificial intelligence techniques," in *Proc. 4th Int. Power Eng. Optim. Conf. (PEOCO)*, Jun. 2010, pp. 38–42.
[129] H. Shayanfar, A. Ghasemi, O. Abedinia, H. Izadfar, and N. Amjady, "Optimal PID power system stabilizer tuning via artificial bee colony," *Tech. Phys. Problems Eng.*, vol. 12, pp. 75–82, 2012.
[130] R. Syahputra and I. Soesanti, "Power system stabilizer model using artificial immune system for power system controlling," *Int. J. Appl. Eng. Res.*, vol. 11, no. 18, pp. 9269–9278, 2016.
[131] B. Changaroon, S. C. Srivastava, and D. Thukaram, "A neural network based power system stabilizer suitable for on-line training—A practical case study for EGAT system," *IEEE Trans. Energy Convers.*, vol. 15, no. 1, pp. 103–109, Mar. 2000.

DEVESH UMESH SARKAR received the B.E. and M.Tech. degrees in electrical engineering from Rashtrasant Tukadoji Maharaj Nagpur University (RTMNU), Nagpur, in 2013 and 2017, respectively. He is currently pursuing the Ph.D. degree with the School of Electrical Engineering, VIT Vellore. From 2017 to 2021, he was an Assistant Professor with the G H Raisoni Institute of Engineering and Technology, Nagpur. His research interests include power system stability, power system optimization, renewable energy source, and the application of artificial intelligence techniques to power systems.

TAPAN PRAKASH (Member, IEEE) received the B.Tech. degree in electrical and electronics engineering from the Maulana Abul Kalam Azad University of Technology (formerly the West Bengal University of Technology), Kolkata, India, in 2010, the M.Tech. degree in power system engineering from the Veer Surendra Sai University of Technology, Burla, Odisha, in 2013, and the Ph.D. degree in electrical engineering from the National Institute of Technology, Raipur, India, in 2019. He has been an Assistant Professor with the School of Electrical Engineering, VIT Vellore, since 2020. His research interests include power system optimization, power system stability, power system control, wide-area monitoring, protection and control of modern power systems, and the application of artificial intelligence techniques to power systems.